



Contents lists available at ScienceDirect

Earth and Planetary Science Letters

www.elsevier.com/locate/epsl



The influence of melt flux and crustal processing on Re–Os isotope systematics of ocean island basalts: Constraints from Galápagos

S.A. Gibson^{a,*}, C.W. Dale^b, D.J. Geist^c, J.A. Day^a, G. Brügmann^d, K.S. Harpp^e^a Dept of Earth Sciences, University of Cambridge, Cambridge, UK^b Dept of Earth Sciences, Durham University, Durham, UK^c National Science Foundation, Earth Sciences Division, 4201 Wilson Blvd., Arlington, VA 22230, USA^d Curt-Engelhorn-Zentrum Archäometrie, Mannheim, Germany^e Geology Department, Colgate University, Hamilton, NY, USA

ARTICLE INFO

Article history:

Received 18 February 2016

Received in revised form 11 May 2016

Accepted 14 May 2016

Available online xxxx

Editor: B. Marty

Keywords:

osmium isotopes

ocean island basalts

Galápagos

mantle plume

crustal contamination

pyroxenite

ABSTRACT

New rhenium–osmium data for high-MgO (>9 wt.%) basalts from the Galápagos Archipelago reveal a large variation in $^{187}\text{Os}/^{188}\text{Os}$ (0.1304 to 0.173), comparable with the range shown by primitive global ocean island basalts (OIBs). Basalts with the least radiogenic $^{187}\text{Os}/^{188}\text{Os}$ occur closest to the Galápagos plume stem: those in western Galápagos have low $^{187}\text{Os}/^{188}\text{Os}$, moderate $^{87}\text{Sr}/^{86}\text{Sr}$, $^{143}\text{Nd}/^{144}\text{Nd}$, $^{206}\text{Pb}/^{204}\text{Pb}$ and high $^3\text{He}/^4\text{He}$ whereas basalts in the south also have low $^{187}\text{Os}/^{188}\text{Os}$ but more radiogenic $^{87}\text{Sr}/^{86}\text{Sr}$, $^{143}\text{Nd}/^{144}\text{Nd}$, $^{206}\text{Pb}/^{204}\text{Pb}$ and $^3\text{He}/^4\text{He}$. Our new Os isotope data are consistent with the previously established spatial zonation of the common global isotopic mantle reservoir “C” and ancient recycled oceanic crust in the mantle plume beneath western and southern parts of Galápagos, respectively.

Galápagos basalts with the most radiogenic $^{187}\text{Os}/^{188}\text{Os}$ (up to 0.1875) typically have moderate MgO (7–9 wt.%) and low Os (<50 pg g^{-1}) but have contrastingly unenriched Sr, Nd and Pb isotope signatures. We interpret this decoupling of chalcophile and lithophile isotopic systems as due to assimilation of young Pacific lower crust during crystal fractionation. Mixing models show the assimilated crust must have higher contents of Re and Os, and more radiogenic $^{187}\text{Os}/^{188}\text{Os}$ (0.32), than previously proposed for oceanic gabbros. We suggest the inferred, exceptionally-high radiogenic ^{187}Os of the Pacific crust may be localised and due to sulfides precipitated from hydrothermal systems established at the Galápagos Spreading Centre.

High $^{187}\text{Os}/^{188}\text{Os}$ Galápagos basalts are found where plume material is being dispersed laterally away from the plume stem to the adjacent spreading centre (*i.e.* in central and NE parts of the archipelago). The extent to which crustal processing influences $^{187}\text{Os}/^{188}\text{Os}$ appears to be primarily controlled by melt flux: as distance from the stem of the Galápagos plume increases, the melt flux decreases and crustal assimilation becomes proportionally greater, accounting for co-variations in Os and $^{187}\text{Os}/^{188}\text{Os}$. The Os concentration threshold below which the $^{187}\text{Os}/^{188}\text{Os}$ of Galápagos basalts are contaminated (100 pg g^{-1}) is higher than the canonical value (<50 pg g^{-1}) assumed for many other global OIBs (*e.g.* for Iceland, Grande Comore and Hawaii). This most likely reflects the low overall melt flux to the crust from the Galápagos plume, which has only a moderate excess temperature and buoyancy flux. Our findings have implications for the interpretation of $^{187}\text{Os}/^{188}\text{Os}$ ratios in other ocean island settings, especially those where large variations in $^{187}\text{Os}/^{188}\text{Os}$ have been linked to heterogeneity in mantle lithology or sulfide populations: the effect of crustal contamination on $^{187}\text{Os}/^{188}\text{Os}$ may be greater than previously recognised, particularly for basalts associated with weak, low melt flux mantle plumes, such as Tristan, Bouvet, Crozet and St Helena.

© 2016 The Author(s). Published by Elsevier B.V. This is an open access article under the CC BY license (<http://creativecommons.org/licenses/by/4.0/>).

1. Introduction

Models invoking lithological heterogeneity of the convecting mantle have been widely adopted to explain elemental and iso-

topic variations in suites of ocean-island basalts (OIBs). Nevertheless, evidence for the extent of this heterogeneity remains contentious, especially the contribution of melts derived from recycled oceanic crust, *i.e.* pyroxenite/eclogite, compared to interaction of melts with the modern oceanic lithosphere. One approach adopted

* Corresponding author.

E-mail address: sally@esc.cam.ac.uk (S.A. Gibson).

to quantify this lithological heterogeneity in OIB source regions utilizes the chalcophile ^{187}Re – ^{187}Os isotopic system, which is distinct from lithophile radiogenic isotopic systems (*i.e.* Sr, Nd, Pb and Hf) because of the large difference in compatibilities of the parent and daughter elements during mantle melting: on a bulk scale, rhenium is moderately incompatible and osmium is strongly compatible (Allègre and Luck, 1980). Decay of ^{187}Re to ^{187}Os causes oceanic crust with high Re/Os (*i.e.* gabbro and basalt) to rapidly develop supra-chondritic $^{187}\text{Os}/^{188}\text{Os}$ isotopic ratios while peridotite melt residues in the lithospheric mantle have low Re/Os and unradiogenic $^{187}\text{Os}/^{188}\text{Os}$. Radiogenic $^{187}\text{Os}/^{188}\text{Os}$ is therefore believed to be a particularly sensitive indicator of ancient recycled crust, and coupled correlations of Os isotopic ratios with those of Sr–Nd–Pb and O have been interpreted as evidence of mixing of melts from peridotite and subducted oceanic crust in the convecting mantle, *e.g.* Reisberg et al. (1993), Hauri et al. (1996), Class et al. (2009), Day et al. (2009).

Osmium is highly-compatible during sulfide fractionation from primary magmas (Burton et al., 2002), and the low Os ($<50\text{ pg g}^{-1}$) of oceanic basalts makes their $^{187}\text{Os}/^{188}\text{Os}$ ratios particularly susceptible to shallow level contamination either by: gabbros in the lower oceanic crust (Os = 55 pg g^{-1} , initial $^{187}\text{Os}/^{188}\text{Os}$ = 0.142; *e.g.* Peucker-Ehrenbrink et al., 2012); interaction with seawater (Os = 0.01 pg g^{-1} , $^{187}\text{Os}/^{188}\text{Os}$ = 1.06; Levasseur et al., 1998) or seawater-altered crust (Gannoun et al., 2007). While upper oceanic crust can acquire a high initial $^{187}\text{Os}/^{188}\text{Os}$ (0.173; Peucker-Ehrenbrink et al., 2003) it typically has a low Os content ($<20\text{ pg g}^{-1}$; Gannoun et al., 2007) and assimilation of young material of this type has a limited effect on the Os isotopic ratios of primitive basalts. The elevated $^{187}\text{Os}/^{188}\text{Os}$ ratios of low Os ($<50\text{ pg g}^{-1}$) oceanic basalts emplaced through young crust ($<25\text{ Ma}$; *e.g.* Iceland, Azores, Pitcairn; Skovgaard et al., 2001; Eisele et al., 2002; Widom and Shirey, 1996) have been attributed to contamination by seawater, assimilation of shallow-level volcanic crust or marine sediments whereas the elevated $^{187}\text{Os}/^{188}\text{Os}$ ratios of low Os ($<50\text{ pg g}^{-1}$) basalts emplaced through ‘old’ oceanic crust have been linked to assimilation of lower crust with highly-radiogenic $^{187}\text{Os}/^{188}\text{Os}$, (*e.g.* Canary Islands and Grande Comore; Class et al., 2009; Day et al., 2010).

Attempts to constrain the composition of recycled material in the convecting mantle have focused on $^{187}\text{Os}/^{188}\text{Os}$ of OIBs with high MgO and Os contents, *e.g.* Bennett et al. (2000), Hauri et al. (1996), Lassiter and Hauri (1998), Dale et al. (2009b), Debaille et al. (2009), Day et al. (2009), Yang et al. (2013). Nevertheless, Harvey et al. (2011) proposed that the broad spectrum of Os and $^{187}\text{Os}/^{188}\text{Os}$ displayed by high Os ($>40\text{ pg g}^{-1}$) OIBs results from sequential melting of different sulphide populations in the convecting mantle, rather than lithological heterogeneities, and the causes of variability in $^{187}\text{Os}/^{188}\text{Os}$ of OIBs therefore remain unclear.

We present the first osmium isotopic ratios, together with Re and Os contents, of recent, high-MgO ($>7\text{ wt.}\%$) basalts in the Galápagos Archipelago. Lavas in this region exhibit large variations in elemental and Sr–Nd–Pb–Hf and He isotopic ratios that are widely believed to result from melting of different reservoirs in the upwelling Galápagos mantle plume (*e.g.* White et al., 1993; Hoernle et al., 2000; Harpp and White, 2001). We combine our Re–Os data with published geochemical analyses of Galápagos basalts, and the results of geophysical investigations, in order to explain regional differences in Os isotopes. Our findings for Galápagos, where detailed information about the underlying crust and plume structure is readily available, provide new constraints on the causes of variability in Os isotope systematics for global oceanic basalts.

2. Summary of the tectonic setting and volcanic activity in Galápagos

The Galápagos hotspot is located 160 km to 250 km south of the Galápagos Spreading Centre (GSC, Fig. 1) and the region is an archetypal example of plume-ridge interaction. The thickness of the Galápagos lithosphere and plume structure have been described in recent investigations and are known in as much, if not greater, detail than any other archipelago. Body wave studies have shown that at depths $>200\text{ km}$ the mantle plume stem resides beneath western Galápagos, which coincides with the region of most active volcanism (Villagómez et al., 2014). At shallower depths material is laterally dispersed from the plume stem towards the GSC. The distribution of historic volcanism on islands between the plume stem and ridge is largely controlled by local variations in lithospheric thickness and a confined NE channel of high-temperature, low-viscosity flow embedded within the normal advection and spreading of the plume (Gibson et al., 2015).

Galápagos volcanism is dominated by mildly alkaline and tholeiitic basalts with sub-ordinate trachytes and rhyolites and activity broadly decreases in age from $<4\text{ Ma}$ in the east of the archipelago to $<1\text{ Ma}$ in the west (White et al., 1993; Geist et al., 2014). The different shield volcanoes on Isabela (Volcans Cerro Azul, Sierra Negra, Alcedo, Darwin, Wolf & Ecuador) and the volcano on Fernandina have the largest calderas, reaching up to 9 km in diameter, and are built on strong, thick lithosphere (Feighner and Richards, 1994). The western volcanoes are supplied by a greater melt flux than currently occurs further east in the archipelago (Geist et al., 1998).

Large regional variations in elemental ratios and Sr, Nd, Pb, Hf and He isotope compositions of Galápagos basalts have been attributed to spatial zonation in the underlying mantle plume (*e.g.* White et al., 1993; Hoernle et al., 2000; Harpp and White, 2001). Harpp and White (2001) identified four isotopically-distinct Galápagos mantle reservoirs: PLUME, which occurs in western Galápagos and resembles the common (“C”) global plume reservoir; Depleted Galápagos Mantle, which is prevalent in central and eastern Galápagos and similar to global depleted mantle; and isotopically enriched Floreana (FLO) and Wolf–Darwin components, found in southern and northwestern Galápagos, respectively. The FLO reservoir is thought to contain ancient, altered oceanic crust that has been isolated in the convecting mantle (Harpp et al., 2014).

3. Methods

Olivine grains were analysed for major and some trace elements using a Cameca SX 100 in the Department of Earth Sciences, University of Cambridge. Whole-rock powders with published major element analyses were digested and then analysed for a range of trace elements on a PerkinElmer Elan DRC II quadrupole Inductively Coupled Plasma (ICP) – Mass Spectrometer (MS) in the Department of Earth Sciences, University of Cambridge and for Sr, Nd and Pb isotopes using a ThermoFinnigan Neptune Multi-collector ICP-MS in the Department of Earth Sciences, Durham University (see Supplementary File Tables S2, S3 and S4 and Gibson et al., 2012 for detailed descriptions of techniques).

Re–Os analyses were undertaken on subsets of samples at the Max-Planck-Institut für Chemie, Mainz in 2000 and in the Department of Earth Sciences, Durham University in 2013. In both cases, 1.5 to 2 g of sample powder was digested and equilibrated with a ^{190}Os – ^{185}Re spike using $\sim 16\text{ mol l}^{-1}\text{ HNO}_3$ and $\sim 12\text{ mol l}^{-1}\text{ HCl}$, in 3:2 or 2:1 proportions (see Supplementary File for further details of digestion techniques). Osmium was loaded onto Pt filaments and analysed as OsO_3^- by negative-thermal ionisation mass spectrometry (N-TIMS) using either a Finnigan MAT 262 (Mainz) or a ThermoFinnigan Triton (Durham). All relevant masses were

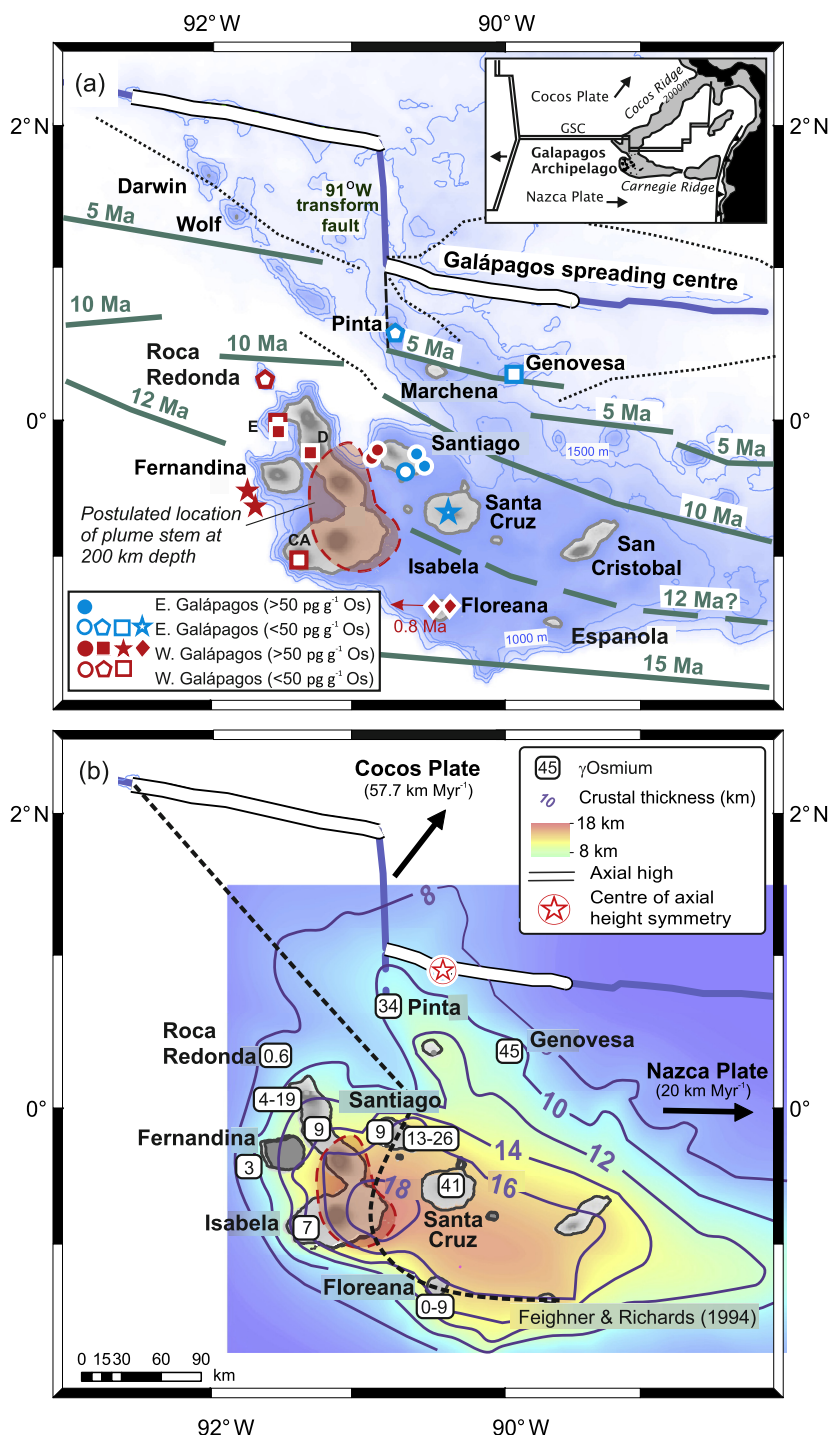


Fig. 1. (a) Distribution of volcanic islands in the Galápagos Archipelago and their relationship to the Galápagos Spreading Centre (GSC), and Galápagos plume stem imaged at a depth of 200 km (Villagómez et al., 2014). At depths shallower than ~150 km plume material is dispersed laterally towards the GSC. (b) Comparison of regional variations of γOs ($[(^{187}\text{Os}/^{188}\text{Os}_{\text{sample}(t)})/(^{187}\text{Os}/^{188}\text{Os}_{\text{PUM}(t)}) - 1] \times 100 \text{ PUM}(t)$) is present-day primitive mantle = 0.1296 (Meisel et al., 2001) in Galápagos basalts with thickness of the Galápagos crust. Dashed black line shows the boundary between thick, strong lithosphere in the west and thin, weak lithosphere in the east of Galápagos (Feighner and Richards, 1994). Bathymetric contours highlight the location of the Galápagos platform and surrounding seamounts. Abbreviations for sample locations on Isabela are as follows: CA, Cerro Azul; D, Volcan Darwin; E, Volcan Ecuador.

measured sequentially using an axial secondary electron multiplier. Data were corrected offline for oxygen isotope interferences, spike-unmixing and mass fractionation (using $^{192}\text{Os}/^{188}\text{Os}$ ratios of 3.082678 (Mainz) and 3.08271 (Durham); these different values are insignificant at the level of precision required and measured on $^{187}\text{Os}/^{188}\text{Os}$. Counts on mass 233 ($^{185}\text{ReO}_3^-$) were typically insignificant for the precision required (<5 counts per second), with no correlation with mass 235, and thus no Re correction was made.

Repeated analyses of Os in-house standard solutions gave average $^{187}\text{Os}/^{188}\text{Os}$ values of 0.10696 ± 0.00005 for 35 pg loads ($n = 73$) and 0.16108 ± 0.00016 for 10 pg aliquots ($n = 23$) at Mainz and Durham, respectively. At Mainz, Re was analysed on a Finnigan MAT 262 N-TIMS. Repeated measurements of a Johnson Matthey Re standard gave an external uncertainty of 0.1% (2 s.d.; $n = 57$). At Durham, Re was measured on a ThermoFinnigan Element 2 ICP-MS. A Romil standard Re solution (1 ng g⁻¹) was analysed during

Table 1
Re–Os compositions of Galápagos basalts.

| Sample No. | Re (pg g ⁻¹) | Os (pg g ⁻¹) | ¹⁸⁷ Os/ ¹⁸⁸ Os | 2σ | γOs | MgO (wt.%) | ⁸⁷ Sr/ ⁸⁶ Sr | ¹⁴³ Nd/ ¹⁴⁴ Nd | ²⁰⁶ Pb/ ²⁰⁴ Pb | ²⁰⁷ Pb/ ²⁰⁴ Pb | ²⁰⁸ Pb/ ²⁰⁴ Pb |
|--|-----------------------------|-----------------------------|--------------------------------------|----------------|-------------|---------------|------------------------------------|--------------------------------------|--------------------------------------|--------------------------------------|--------------------------------------|
| Western Galápagos | | | | | | | | | | | |
| R. Redonda R9512 ^a | 84.3 | 32.2 | 0.13037 | 0.00051 | 0.60 | 17.44 | 0.703217 | 0.512951 | 19.336 | 15.612 | 39.076 |
| Fernandina AHA D25A ^a | 457 | 69.4 | 0.13412 | 0.00014 | 3.49 | 11.09 | 0.703249 | 0.512929 | 19.055 | 15.556 | 38.706 |
| Fernandina AHA 32D ^a | 910 | 149 | 0.13291 | 0.00007 | 2.55 | 11.5 | 0.703218 | 0.512933 | 19.065 | 15.563 | 38.726 |
| Fernandina AHA 32D (repeat) ^a | 709 | 142 | 0.13249 | 0.00011 | 2.23 | | | | | | |
| V. Ecuador E95 10 ^a | 265 | 31.6 | 0.13441 | 0.00023 | 3.71 | 9.36 | | | | | |
| V. Ecuador E95-02 ^b | | 109 | 0.15393 | 0.00051 | 18.8 | 12.29 | 0.703271 | 0.512934 | 19.289 | 15.601 | 39.037 |
| V. Ecuador E97-134 ^b | | 83.8 | 0.15340 | 0.00029 | 18.4 | 10.74 | 0.703050 | 0.512956 | 19.209 | 15.592 | 38.888 |
| Cerro Azul G192-11A ^a | 478 | 36.5 | 0.13918 | 0.00020 | 7.39 | 10.66 | 0.703302 | 0.512953 | 19.377 | 15.561 | 38.993 |
| V. Darwin E-64 ^b | | 552 | 0.13803 | 0.00018 | 6.50 | 9.44 | | | | | |
| Southern Galápagos | | | | | | | | | | | |
| Floreana FL03-20 ^a | 284 | 87.7 | 0.14109 | 0.00009 | 8.87 | 12.85 | 0.703485 | 0.512951 | 20.061 | 15.658 | 39.782 |
| Floreana FL03-106 ^a | 253 | 109 | 0.13014 | 0.00013 | 0.42 | 12.91 | 0.703447 | 0.513001 | 19.886 | 15.648 | 39.604 |
| Floreana E-110 ^b | | 86.1 | 0.13853 | 0.00025 | 6.89 | 11.07 | 0.703600 | 0.512975 | 19.785 | 15.636 | 39.516 |
| Floreana FL-3 ^b | | 154 | 0.13471 | 0.00045 | 3.94 | 12.79 | 0.703660 | 0.512905 | 20.002 | 15.657 | 39.739 |
| Central Galápagos | | | | | | | | | | | |
| W. Santiago 08DSG33 ^a | 150 | 50.6 | 0.15951 | 0.00020 | 23.1 | 9.37 | | | 19.129 | 15.588 | 38.785 |
| W. Santiago 07DSG61 ^a | 314 | 73.6 | 0.14157 | 0.00012 | 9.23 | 10.73 | 0.703009 | 0.513019 | 18.981 | 15.582 | 38.632 |
| W. Santiago E-76 ^b | | 227 | 0.16144 | 0.00036 | 24.6 | 14.34 | 0.702860 | 0.513002 | 19.050 | 15.580 | 38.656 |
| W. Santiago E-20 ^b | | 59.2 | 0.15322 | 0.00032 | 18.2 | 9.89 | 0.702940 | 0.512980 | 19.022 | 15.582 | 38.726 |
| E. Santiago 07DSG72 ^a | 498 | 52.5 | 0.15538 | 0.00016 | 19.9 | 9.83 | 0.702819 | 0.513057 | 18.690 | 15.535 | 38.263 |
| E. Santiago 08DSG42 ^a | 277 | 15.7 | 0.16321 | 0.00044 | 25.9 | 10.37 | 0.702926 | 0.513040 | 18.718 | 15.535 | 38.275 |
| E. Santiago 08DSG16 ^a | 157 | 34.2 | 0.14707 | 0.00023 | 13.5 | 9.19 | 0.702864 | 0.513057 | 18.749 | 15.546 | 38.329 |
| E. Santiago 08DSG04 ^a | 327 | 49.9 | 0.15453 | 0.00016 | 19.2 | 10.09 | 0.702752 | 0.513073 | 18.594 | 15.535 | 38.175 |
| Santa Cruz E-1 ^b | | 21.2 | 0.18303 | 0.00047 | 41.2 | 10.43 | 0.702630 | 0.513077 | 18.514 | 15.520 | 38.048 |
| North East Galápagos | | | | | | | | | | | |
| Genovesa E-169 ^b | | 21.3 | 0.18751 | 0.00078 | 44.7 | 8.09 | 0.702720 | 0.513127 | 18.387 | 15.511 | 37.941 |
| Pinta P-24 ^b | | 46.0 | 0.17318 | 0.00035 | 33.6 | 7.23 | 0.703130 | 0.512943 | | | |

Analyses in bold are from this work. Sources of additional data are given in Table S4.

Because of the relatively young age of basalts from western Galápagos (<1 Ma) and imprecise but young ages (<4 Ma) for basalts from the rest of the archipelago we have not corrected measured ¹⁸⁷Os/¹⁸⁸Os for in-growth of ¹⁸⁷Os. This does not significantly affect our findings as the correction for in-growth of ¹⁸⁷Os to a 4 Ma sample with a Re/Os of ~18 (17 ppt Os and 300 ppt Re) and ¹⁸⁷Os/¹⁸⁸Os of 0.15 would involve a difference in ¹⁸⁷Os/¹⁸⁸Os of only ~0.006.

^a Denotes Re–Os analyses performed at the University of Durham.

^b Analyses at the University of Mainz. Good reproducibility is demonstrated by duplicate analysis of basalt AHA-32D, for which the standard deviation (2σ) on the ¹⁸⁷Os/¹⁸⁸Os and Os concentrations were <0.5% and 7%, respectively. The variation in Re content was greater, at 35% (Table 1). Repeat analyses of the reference material TDB-1 provide a longer-term test of reproducibility which included the second analytical session (Durham): This gave a standard deviation (2σ) of ~20% for Os content and 4% for Re (n = 4), giving rise to a 20% variation in ¹⁸⁷Os/¹⁸⁸Os due to ingrowth over >1000 Ma.

each session to quantify the mass fractionation and a correction applied; this effect was always <2% on the sample concentration. Total procedural blanks for Mainz were 0.2–1.5 pg Os, 0.1–0.5 pg Re (n = 8) with ¹⁸⁷Os/¹⁸⁸Os of 0.14–0.17 and Durham 0.25–1.9 pg Os, 0.5–1.2 pg Re (n = 3) with ¹⁸⁷Os/¹⁸⁸Os of 0.145–0.17.

4. Osmium isotope ratios of Galápagos basalts

4.1. Samples

Twenty-three samples, encompassing the full Sr-, Nd- and Pb-isotopic range displayed by Galápagos basalts, were analysed for ¹⁸⁷Os/¹⁸⁸Os. We focused on the most primitive samples available from each island, specifically those with high bulk-rock Ni contents because of the similar behaviour of Os and Ni during crystal fractionation, albeit due to compatibility in different phases (Os in sulfides and Cr-spinel, Ni in silicate phases Burton et al., 2000). In most cases we analysed samples with >200 μg g⁻¹ Ni, >9 wt.% MgO and Mg# (Mg/Mg + Fe) = 0.6, exceptions were islands in NE Galápagos where the most primitive basalts have <100 μg g⁻¹ Ni, 7 to 9 wt.% MgO and Mg# = 0.5 to 0.63 (Fig. S1).

Ni and Cu sulphides are rare in Galapagos basalts but when present occur as either ~10 μm inclusions in olivine or as ~10 μm rounded globules in the matrix glass (Fig. S2). In the samples from western and southern Galápagos (Fernandina, Isabela, Roca Redonda, Floreana) olivine occurs as both euhedral phenocrysts and large, strained macrocrysts with undulose extinction but in central (Santiago) and NE Galápagos (Pinta and Genovesa) it is predomi-

nantly present as euhedral phenocrysts (Table S1). Since olivine in Galápagos basalt is associated with Cr-spinel or sulfide inclusions, we have examined the possible effects of loss and accumulation of this phase on bulk-rock compositions. Co-variations between bulk-rock Mg# and forsterite content of the olivines (Table S2) suggest they are in equilibrium with the host magma at crustal pressures (Fig. S3) and, importantly, the samples (with the exception of R9512) have not undergone extensive loss or accumulation of olivine.

4.2. Os and Re contents of Galápagos basalts

Osmium contents of Galápagos basalts range from 15 to 552 pg g⁻¹ (Table 1) and generally exhibit a positive correlation with MgO, Ni and Cr (Fig. 2). Exceptions are: the Roca Redonda sample (R9512) that has low Os (32 pg g⁻¹) given its high MgO (17.4 wt.%), Ni (510 μg g⁻¹) and Cr contents (625 μg g⁻¹); and a Volcan Darwin sample (E64) that has high Os (553 pg g⁻¹) and modest MgO (9.44 wt.%; Table 1, Table S4). The co-variation of Os with MgO, Ni and Cr shown by Galápagos basalts is more systematic than has been observed for lavas from other OIBs and we attribute the relationship between Ni, MgO and Os to coupled crystallization of silicates and sulfides. We have used our whole-rock data with fractional crystallisation equations to calculate a bulk partition coefficient (D) for an early crystallising assemblage of olivine, Cr-spinel and sulfide. The best fit to our observed data is for a D_{Os} of ~15 (Fig. 2). This is much greater than the estimated D_{Os}^{olivine} of 0.51 (Burton et al., 2002) and represents preferential

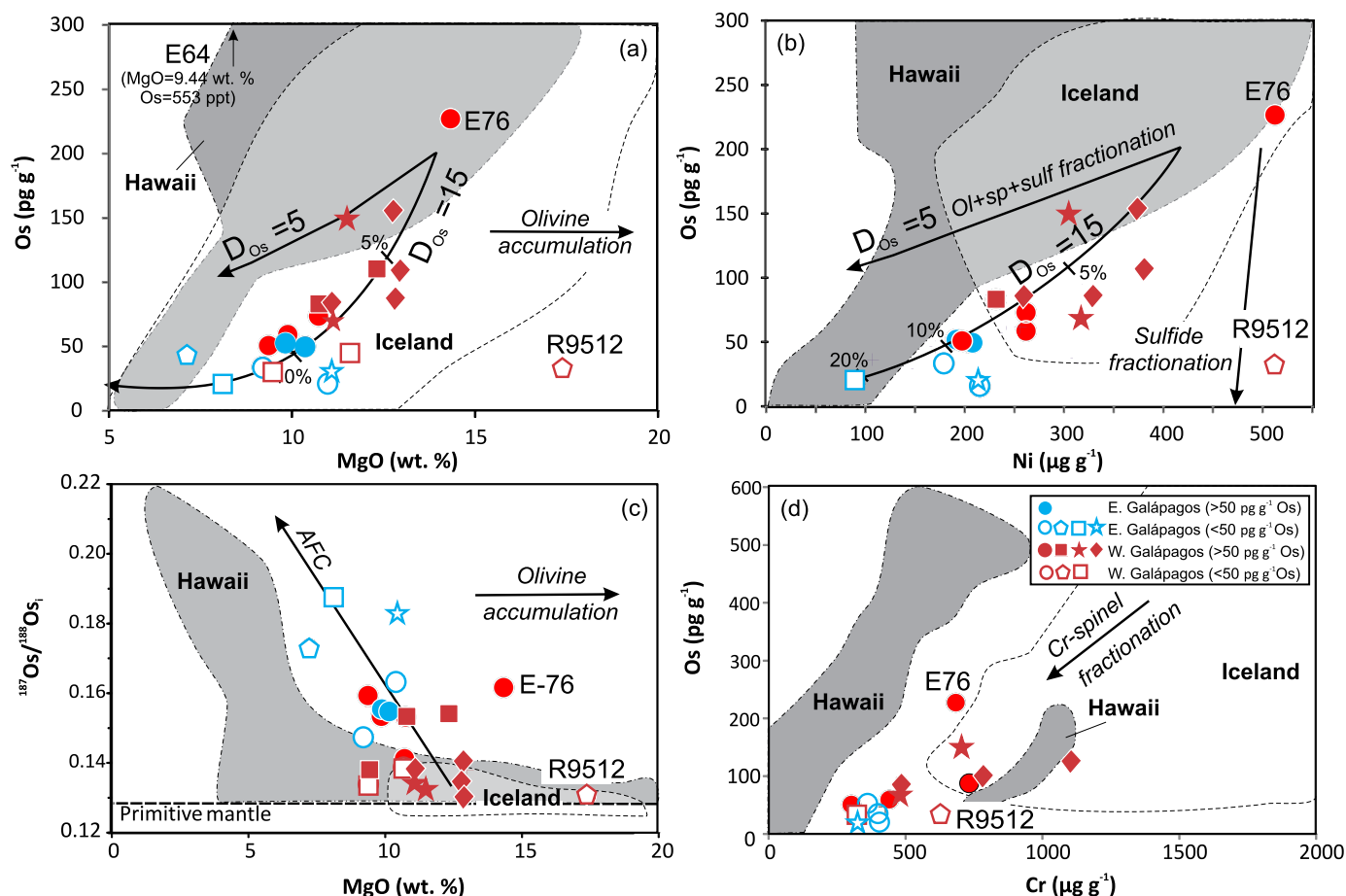


Fig. 2. Variation of (a) MgO and (b) Ni with Os; (c) MgO with $^{187}\text{Os}/^{188}\text{Os}$ and (d) Cr with Os in Galápagos basalts. In (a) solid curve shows predicted crystal fractionation trend for a melt similar to submarine Fernandina picrite AHA19A, which has 14 wt.% MgO and 419 $\mu\text{g g}^{-1}$ Ni (Geist et al., 2006) and an estimated Os content of 200 pg g^{-1} . Fractionation curves were calculated using the thermodynamic modelling program Petrolog3 (Danyushevsky and Plechov, 2011). For an early crystallising assemblage of olivine + Cr spinel + sulfide a D value for Os of 15, together with D_{Os} clinopyroxene = 0.3 and D_{Os} plagioclase = 0.3, provided the best fit to the observed whole-rock data. Tick marks at 5%, 10% and 20% are for fractionation of olivine + Cr spinel + sulfide. In (b) D values for Ni are from Beattie et al. (1991). $^{187}\text{Os}/^{188}\text{Os}$ for primitive mantle is from Meisel et al. (2001). Data sources are given in a Supplementary File. Specific symbols refer to locations given in Fig. 1.

partitioning of Os into sulfides, rather than simply into olivine, during the early stages of fractional crystallisation (e.g. Jackson and Shirey, 2011).

Galápagos basalts exhibit a relatively large variation in Re (80 to 910 pg g^{-1} , Table 1), which displays a scattered correlation with both MgO and Ni contents. The highest Re contents occur in submarine Fernandina basalts (western Galápagos); the wide range in Re contents of other Galápagos basalts – and variability with respect to Cu (which has similar compatibility Fig. S4) – may be due to Re loss during sub-aerial degassing (Bennett et al., 2000).

4.3. $^{187}\text{Os}/^{188}\text{Os}$ characteristics of Galápagos basalts

The $^{187}\text{Os}/^{188}\text{Os}$ compositions of Galápagos basalts vary from 0.130 to 0.1875 ($\gamma_{\text{Os}} = 0.5$ to 45, where $\gamma_{\text{Os}} = ([^{187}\text{Os}/^{188}\text{Os}_{\text{sample}}]/[^{187}\text{Os}/^{188}\text{Os}_{\text{PUM}}] - 1) \times 100$ and PUM(t) is present-day primitive upper mantle = 0.1296; Meisel et al., 2001; Table 1). Despite local and sometimes intra-island variations in $^{187}\text{Os}/^{188}\text{Os}$, e.g. Volcan Ecuador (Table 1), there is a broadly-systematic regional variation in Os isotopic ratios (Fig. 1b). Recently erupted basalts (<1 Ma) with relatively unradiogenic $^{187}\text{Os}/^{188}\text{Os}$ ratios occur in: (i) western Galápagos (Roca Redonda and Fernandina), near the leading edge of the Galápagos plume and on the platform margins and (ii) 1.5 Ma to 779 ka flows on Floreana which, assuming a velocity of the Nazca plate of 20 km Myr^{-1} , would have been located

near the southern margin of the plume stem at the time of their emplacement (Harpp et al., 2014).

The most radiogenic $^{187}\text{Os}/^{188}\text{Os}$ ratios occur in recent basalts from central and NE Galápagos (Fig. 1b). High $^{187}\text{Os}/^{188}\text{Os}$ ratios were measured in basalts with $>50 \text{ pg g}^{-1}$ Os from Santiago (up to 0.155) and northern Isabela (Volcan Ecuador; 0.153). Even more radiogenic $^{187}\text{Os}/^{188}\text{Os}$ ratios (up to 0.1875) were measured in basalts with $<50 \text{ pg g}^{-1}$ Os on Genovesa, Pinta and Santa Cruz. While $^{187}\text{Os}/^{188}\text{Os}$ exhibits a broad inverse relationship with MgO and Os content (Fig. 2), we note that Galápagos lavas with similar MgO contents exhibit a large inter-island variation in $^{187}\text{Os}/^{188}\text{Os}$. For example, Fernandina submarine basalts with ~11 wt.% MgO have $^{187}\text{Os}/^{188}\text{Os}$ ratios of 0.133, while <1Ma basalts from Isla Santiago (70 km east in central Galápagos) with comparable MgO and Os contents have $^{187}\text{Os}/^{188}\text{Os}$ ranging from 0.142 to 0.163 (Table 1).

The combined relatively unradiogenic $^{187}\text{Os}/^{188}\text{Os}$ (0.1329–0.1342), moderate $^{143}\text{Nd}/^{144}\text{Nd}$ (0.51292–0.51296) and $^{206}\text{Pb}/^{204}\text{Pb}$ (19.05–19.1), high $^3\text{He}/^4\text{He}$ (up to 29 R/Ra) and $\delta^{18}\text{O}$ ($5.6 \pm 1\text{‰}$) of Fernandina basalts (White et al., 1993; Geist et al., 1998; Harpp and White, 2001; Kurz et al., 2009) support the hypothesis that their parental melts are derived from “C” like, primitive, lower mantle (Fig. 3) and suggests that their Os systematics are most likely controlled by sulfide in this mantle source (cf. Harvey et al., 2011). Similarly, we interpret the unradiogenic $^{187}\text{Os}/^{188}\text{Os}$ (0.1304) of the Roca Redonda picrite as evidence that, despite significant accumulated olivine (Fo_{83.3}; Vidito et al., 2013) and ap-

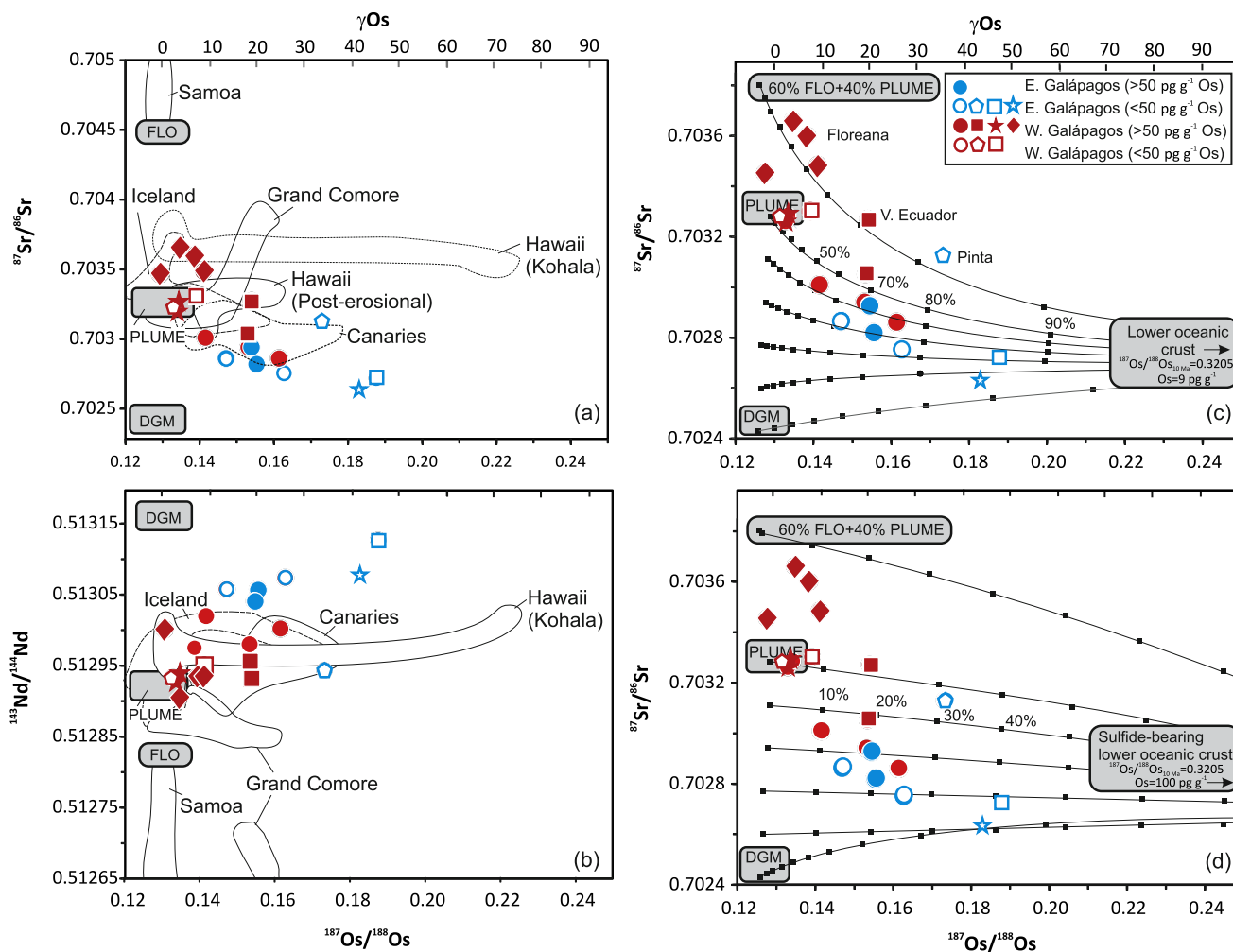


Fig. 3. (a) and (b) Co-variations in Os-, Sr- and Nd-isotopes in Galápagos basalts and global ocean islands. Compositions of Galápagos mantle reservoirs are as follows: PLUME, $^{187}\text{Os}/^{188}\text{Os} = 0.1296$, $^{87}\text{Sr}/^{86}\text{Sr} = 0.70328$, $^{143}\text{Nd}/^{144}\text{Nd} = 0.51289$; Depleted Galápagos Mantle (DGM), $^{187}\text{Os}/^{188}\text{Os} = 0.127$, $^{87}\text{Sr}/^{86}\text{Sr} = 0.70243$, $^{143}\text{Nd}/^{144}\text{Nd} = 0.51317$; Floreana (FLO) $^{187}\text{Os}/^{188}\text{Os} = 0.147$, $^{87}\text{Sr}/^{86}\text{Sr} = 0.70450$, $^{143}\text{Nd}/^{144}\text{Nd} = 0.51283$. The enriched Wolf-Darwin component, which is prevalent in islands northwest of the main Galápagos platform, makes a negligible contribution to basalts analysed for $^{187}\text{Os}/^{188}\text{Os}$. Note that the $^{187}\text{Os}/^{188}\text{Os}$ of PLUME and DGM are assumed to be the same as primitive and MORB-source mantle, respectively (Meisel et al., 2001; Gannoun et al., 2007). Mixing curves at 20% increments between PLUME, DGM, FLO and lower crust with the $^{187}\text{Os}/^{188}\text{Os}$ composition of Blusztajn et al. (2000) are shown in (c) and sulfide-bearing lower oceanic crust for Galápagos with the Sr composition of Hart et al. (1999) are shown in (d). Note that the effect of assimilation on Os isotopes is more significant than on $^{87}\text{Sr}/^{86}\text{Sr}$, which is consistent with the Sr–Nd isotope variations primarily reflecting mantle source heterogeneity. Data are from: Table 1 and sources are given in a Supplementary File. Specific symbols refer to locations given in Fig. 1.

parent stalling of the parental melt in the crust, it has reached the surface with little crustal interaction.

Harpp and White (2001) showed that in Sr–Nd- and Pb-isotopic space the FLO (Floreana) mantle reservoir in southern Galápagos lies on a hyperbolic mixing curve between PLUME and global subducted, altered 2 Ga oceanic crust (HIMU). The $^{187}\text{Os}/^{188}\text{Os}$ ratios of Floreana basalts vary from 0.130–0.141. The sample with the least radiogenic $^{187}\text{Os}/^{188}\text{Os}$ (0.13014; FLO3-106) has moderately radiogenic $^{143}\text{Nd}/^{144}\text{Nd}$ (0.5130) and $^{206}\text{Pb}/^{204}\text{Pb}$ (19.89). By extrapolating to the previously estimated $^{206}\text{Pb}/^{204}\text{Pb}$ of the FLO endmember (21.2; Harpp and White, 2001) in Fig. 4 we infer this reservoir has a $^{187}\text{Os}/^{188}\text{Os}$ ratio of 0.147. The two most radiogenic Floreana basalts (E110 and FL-3; $^{187}\text{Os}/^{188}\text{Os} = 0.139$ –0.141) have similar $^{206}\text{Pb}/^{204}\text{Pb}$ ratios (19.8–20) and plot on a mixing curve between melts of Galápagos FLO and PLUME reservoirs and an endmember with high $^{187}\text{Os}/^{188}\text{Os}$.

Surprisingly, the Os isotopic ratios of central and NE Galápagos basalts exhibit broadly negative and positive correlations with Sr and Nd isotopic ratios, respectively (Fig. 3). These basalts have MORB-like Sr and Nd isotopic ratios, with unradiogenic Pb, but

their $^{187}\text{Os}/^{188}\text{Os}$ are more radiogenic (0.147–0.188) than present-day MORB (0.126–0.14; Gannoun et al., 2007), primitive upper mantle (0.1296; Meisel et al., 2001) and global OIBs derived from the “C” plume reservoir (0.1245–0.1314; Tejada et al., 2015). Similar relationships between Pb and Os isotopic ratios of global OIBs with >30–40 pg g^{-1} Os have been interpreted as mixing of primitive enriched “C”-like plume melts with ancient recycled pyroxenite (e.g. Lassiter and Hauri, 1998; Skovgaard et al., 2001; Day et al., 2009): Fig. 4. Although this interpretation cannot be completely ruled out, we note that the combined unradiogenic Sr-, Pb- and radiogenic Nd-isotope characteristics of some central and NE Galápagos basalts are not consistent with a significant contribution from ancient recycled oceanic crust. Melting of this mantle reservoir would result in basalts with combined radiogenic $^{206}\text{Pb}/^{204}\text{Pb}$ and $^{187}\text{Os}/^{188}\text{Os}$ ratios, similar to those that we have identified at Floreana (Fig. 4). Thus, the origin of these isotopic covariations in global OIB remains unclear. Here we present an alternative mechanism for generating the radiogenic Os signature, based on a greater understanding of magma flux and lithospheric structure at Galápagos.

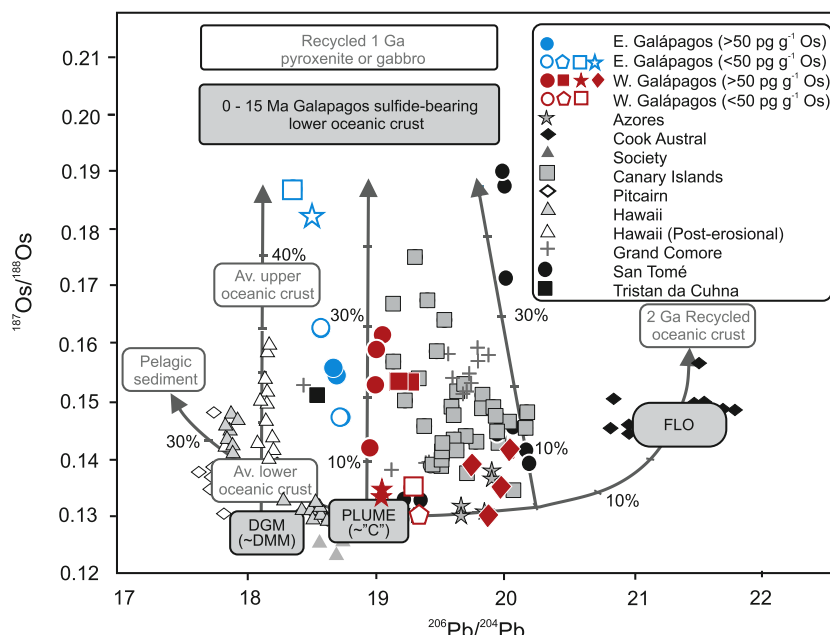


Fig. 4. Plot of $^{206}\text{Pb}/^{204}\text{Pb}$ versus $^{187}\text{Os}/^{188}\text{Os}$ for Galápagos basalts together with published analyses for global OIBs. On the basis that FLO is a mixture of PLUME and HIMU-like mantle and has a $^{206}\text{Pb}/^{204}\text{Pb}$ of 21.2 (Harpp and White, 2001) we infer the $^{187}\text{Os}/^{188}\text{Os}$ of the FLO reservoir to be 0.147. Bulk mixing curves were calculated using reservoirs with the following values: lower crust (Os = 100 pg g^{-1} , $^{187}\text{Os}/^{188}\text{Os}$ = 0.32 (see text for discussion) and $^{206}\text{Pb}/^{204}\text{Pb}$ = 17.8 to 20); DGM, Depleted Galápagos Mantle ($^{187}\text{Os}/^{188}\text{Os}$ = 0.127, $^{206}\text{Pb}/^{204}\text{Pb}$ = 18.1); PLUME ($^{187}\text{Os}/^{188}\text{Os}$ = 0.1296, $^{206}\text{Pb}/^{204}\text{Pb}$ = 18.9); 2 Ga recycled oceanic crust (Os = 3.1 pg g^{-1} , $^{187}\text{Os}/^{188}\text{Os}$ = 2.74, Pb = 0.9 ng g^{-1} , $^{206}\text{Pb}/^{204}\text{Pb}$ = 21.53). Melts from these mantle reservoirs were assumed to have 200 pg g^{-1} Os and 0.8 ng g^{-1} Pb. Those from sulfide-bearing Pacific lower oceanic crust were assumed to have 100 pg g^{-1} Os and 0.5 ng g^{-1} Pb. Data sources are provided in a Supplementary File. Specific symbols refer to locations given in Fig. 1.

5. What is the cause of large inter-island variations in Os isotope ratios of Galápagos basalts?

Variable extents of melting of different sulfide populations in the convecting mantle (Harvey et al., 2011), could generate variations in $^{187}\text{Os}/^{188}\text{Os}$ that are decoupled from those of lithophile isotopes in Galápagos basalts. For example, higher degree melting close to the plume stem might result in more Os-rich melts with less radiogenic Os, than more distal melts. Such a model could account for the variable $^{187}\text{Os}/^{188}\text{Os}$ in basalts with similar Os contents close to the plume stem, but not the wide range of $^{187}\text{Os}/^{188}\text{Os}$ displayed by Galápagos basalts as a whole. On a plot of $^{206}\text{Pb}/^{204}\text{Pb}$ versus $^{187}\text{Os}/^{188}\text{Os}$, Galápagos basalts exhibit a broad negative correlation (Fig. 4), which implies they contain melts with high $^{187}\text{Os}/^{188}\text{Os}$ and low $^{206}\text{Pb}/^{204}\text{Pb}$. The source of the radiogenic Os must have high time-averaged Re/Os and the most plausible explanation is that it is either (i) ancient subducted oceanic crust in the convecting mantle, or (ii) 5 to 15 Ma Pacific crust (Fig. S5).

While the Sr-, Nd-, Hf-, Pb- and Os-isotopic ratios of Floreana basalts are consistent with at least some ancient subducted material undergoing melting in the Galápagos plume, a number of lines of evidence suggest that $^{187}\text{Os}/^{188}\text{Os}$ of other Galápagos magmas result instead from assimilation of Pacific crust. First, the regional variability in $^{187}\text{Os}/^{188}\text{Os}$ shows a negative correlation ($r = -0.61$) with proposed lithological variations (i.e., pyroxenite or peridotite) in the Galápagos plume based on the parameterisation of elemental concentrations (Mg, Fe, Ni and Mn) in olivine (Vidito et al., 2013, Figs. S6 and S7). Second, Galápagos basalts display broad systematic variations in $^{187}\text{Os}/^{188}\text{Os}$ with indices of crystal fractionation, e.g. MgO ($r = -0.87$) and Ni ($r = -0.83$), implying that the variability in $^{187}\text{Os}/^{188}\text{Os}$ post-dates melt generation in the mantle. Finally, the spatial zonation in Os isotopes of Galápagos basalts can be directly linked to variations in the melt flux from the Galápagos plume in to the crust (see below).

The sensitivity of $^{187}\text{Os}/^{188}\text{Os}$ ratios of oceanic basalts to assimilation of crustal material is highly dependent upon magmatic Os contents (Fig. S8). Previous investigations have shown that OIBs

with 30 to 50 pg g^{-1} Os are especially susceptible (e.g. Reisberg et al., 1993; Eisele et al., 2002; Class et al., 2009). Nevertheless, not all low-Os Galápagos basalts have high $^{187}\text{Os}/^{188}\text{Os}$ and, as we described above, the sample with the least radiogenic $^{187}\text{Os}/^{188}\text{Os}$ (Roca Redonda) has one of the lowest Os contents.

6. The origin of regional variations in crustal contamination of Galápagos plume-derived melts

Our conclusion that radiogenic Os isotope ratios of Galápagos basalts primarily reflect crustal assimilation is consistent with findings from whole-rock (Saal et al., 2007) and melt-inclusion data (Peterson et al., 2014). Saal et al. (2007) noted that some Galápagos basalts erupted east of 91°W have positive Sr anomalies on normalised multi-element plots, and suggested they are evidence of crustal contamination in basalts erupted distal to the present-day plume stem. Our new Os isotope data show, however, that some basalts which lack a positive Sr anomaly have radiogenic $^{187}\text{Os}/^{188}\text{Os}$ and may also have assimilated oceanic crust, such as alkaline basalts on western Santiago (Figs. 5 and S5). Their relatively high Sr, Pb, and Eu concentrations obscure any evidence of a crustal contribution on normalised multi-element plots, but osmium isotopes are a more sensitive indicator of assimilation. Because of the multiple causes of Sr variability in Galápagos basalts the overall correlation of Sr with $^{187}\text{Os}/^{188}\text{Os}$ is weak (Fig. S6).

The variability in $^{187}\text{Os}/^{188}\text{Os}$ of Galápagos basalts does not directly correlate with age and hence thickness of the underlying Pacific crust but subtle regional variations in lower crust composition potentially exert a control on the crustal processing of plume-derived melts (Figs. 1 and S5). Much of the Galápagos platform is underlain by crust more than twice as thick as that currently forming on the GSC above ambient temperature mantle (Feighner and Richards, 1994; Canales et al., 2002). The thickest Galápagos crust

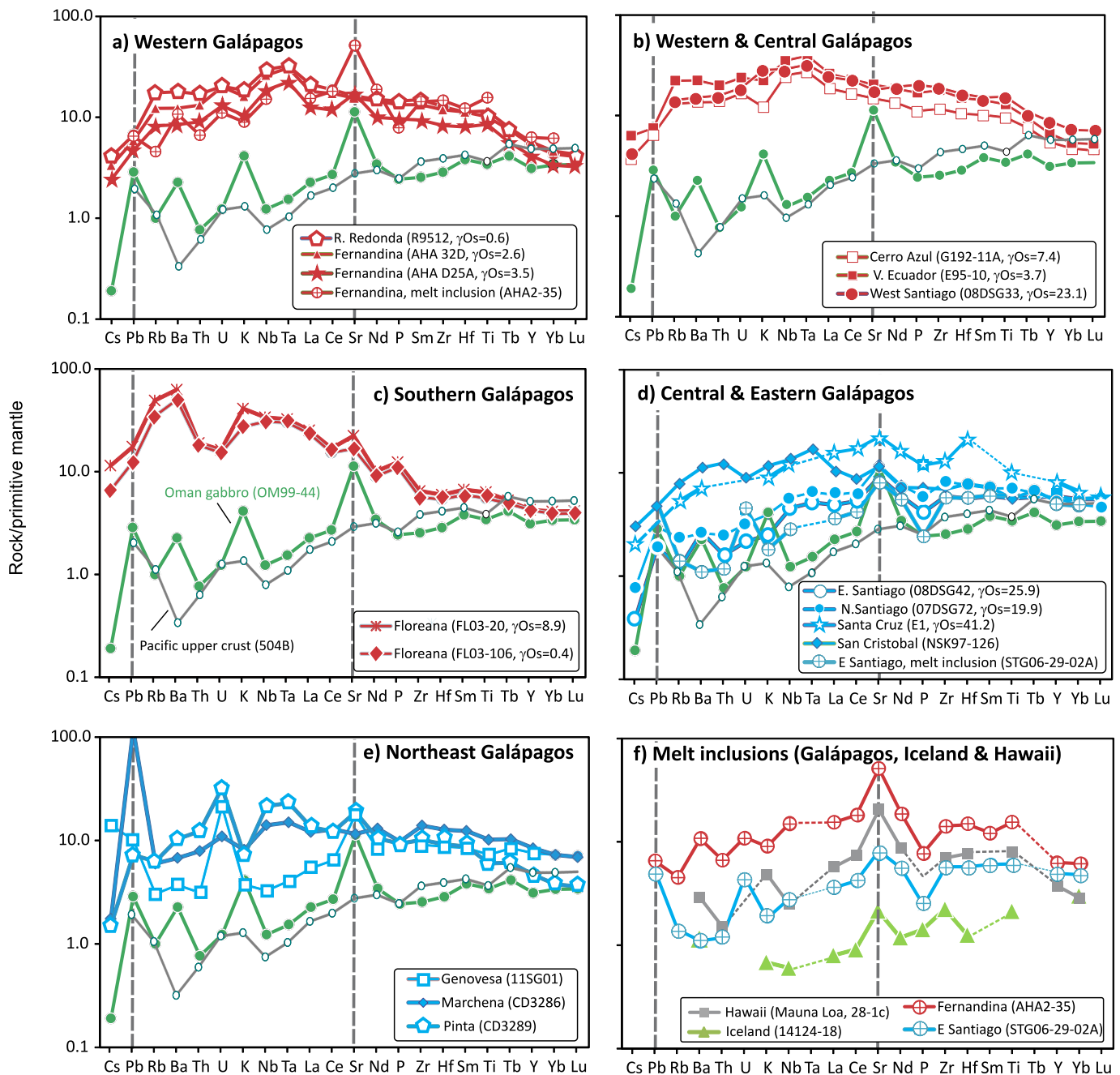


Fig. 5. Comparison of primitive-mantle-normalised multi-element patterns of basalts from western (red symbols) and eastern Galápagos (blue symbols) with lower oceanic crust (Oman gabbro, [Peucker-Ehrenbrink et al., 2012](#)) and upper oceanic crust (504B, [Bach et al., 2003](#)). The positive Sr anomaly in melt inclusions from E. Santiago and Fernandina has been interpreted as evidence of diffusive interaction of a depleted melt with a plagioclase-rich cumulate in the oceanic crust ([Peterson et al., 2014](#)). Analyses of melt inclusions from global OIBs believed to have melt contributions from recycled oceanic crust (Hawaii) and underlying young crust (Galápagos and Iceland) are shown for comparison. Osmium isotopic data are given where known for specific samples. Data are from: [Table 1](#), Supplementary Table 1 and sources are given in a Supplementary File. (For interpretation of the references to colour in this figure legend, the reader is referred to the web version of this article.)

(up to 18 km) occurs beneath the western part of the platform, above the present-day plume stem ([Feighner and Richards, 1994](#)). The lower 6–8 km of this is likely dominated by mafic and ultramafic intrusions emplaced in ridge-generated crust ([Richards et al., 2013](#)). Away from the plume stem and east of $\sim 91^\circ\text{W}$ ([Fig. 1](#)) the crust is thinner (8–12 km) and weaker ([Feighner and Richards, 1994](#)). The young (~ 5 Ma) crust beneath the northeast of the archipelago was created when the Galápagos plume was located near the GSC and most likely consists of wehrlitic and gabbroic material, similar to that thought to form the basement of the Co-cos and Carnegie ridges ([Sallarès et al., 2003](#)).

6.1. Modelling the effects of crustal processing on $^{187}\text{Os}/^{188}\text{Os}$ of Galápagos magmas

With the exception of E64 (Volcan Darwin) and R9512 (Roca Redonda), Galápagos basalts fall on predicted fractional crystallisation trends on MgO versus Os plots ([Fig. 2](#)), and show no evidence of having accumulated an Os-rich phase. We have therefore used the equations of [Nishimura \(2012\)](#) to model assimilation fractional crystallisation (AFC) and thereby assess the effects of crustal interaction on both Os contents and $^{187}\text{Os}/^{188}\text{Os}$ ratios of Galápagos basalts ([Fig. 6](#)). While our AFC models assume a bulk D_{Os} of 15, and that whole-rock compositions are representative of

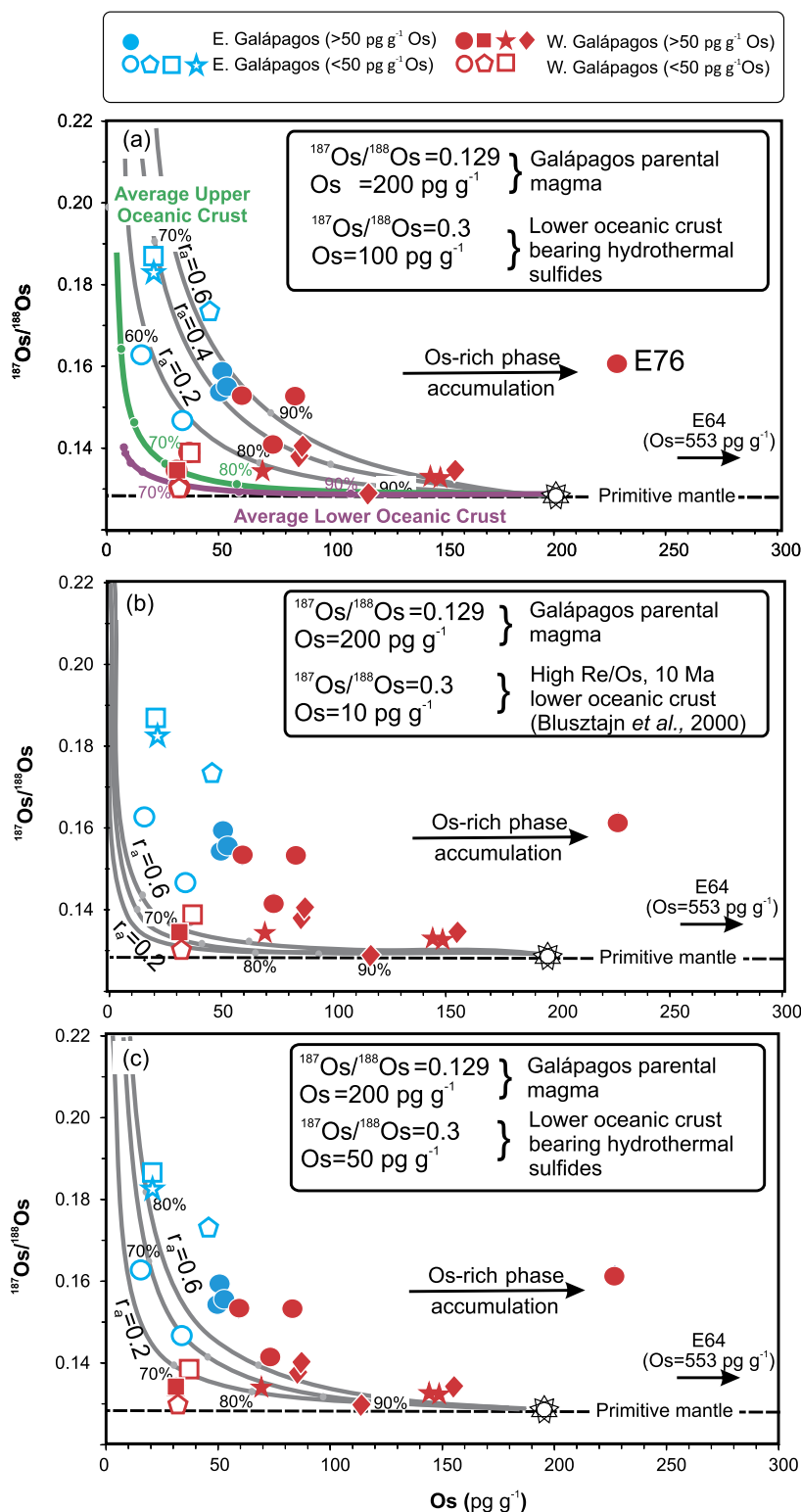


Fig. 6. Variation of Os and $^{187}\text{Os}/^{188}\text{Os}$ in Galápagos basalts. Data are from Table 1. Curves show the results of Assimilation Fractional Crystallisation modelling (Nishimura, 2012) of a primitive Galápagos magma with 200 pg g^{-1} Os and $^{187}\text{Os}/^{188}\text{Os}$ of 0.129. (a) shows the effects of assimilating average upper and lower oceanic crust and also hypothetical lower oceanic crust containing hydrothermal sulfides and 100 pg g^{-1} Os; (b) shows the effects of assimilating high Re/Os 10 Ma lower crust with 10 pg g^{-1} Os (Blusztajn et al., 2000) and (c) shows the effect of assimilating hypothetical lower oceanic crust containing hydrothermal sulfides and 50 pg g^{-1} Os. Bulk D_{Os} was set to 15 for the early crystallising assemblage of olivine + Cr spinel + sulfide (see text for discussion). The ratio of assimilation to crystal fractionation (r_a) and the % mass of the residual magma relative to the initial mass are shown on all plots. The Os contents and $^{187}\text{Os}/^{188}\text{Os}$ for average upper and lower oceanic crust are from Peucker-Ehrenbrink et al. (2003, 2012). Specific symbols refer to locations given in Fig. 1.

parental melts (Section 3), they are compromised by $^{187}\text{Re}/^{188}\text{Os}$ and $^{187}\text{Os}/^{188}\text{Os}$ ratios of oceanic crust for which published data are limited (Gannoun et al., 2016).

Young upper crust in the Nazca plate as sampled by DSDP 504B can acquire high initial $^{187}\text{Os}/^{188}\text{Os}$ (0.173) but has a low mean Os content (23 pg g^{-1} ; Peucker-Ehrenbrink et al., 2003) and assimilation of such material would have little effect on the Os isotopic ratios of Galápagos basalts with 100's of pg g^{-1} Os (Fig. 6a). DSDP 504B did not penetrate lower crust, and there are no Re–Os data for gabbros from here or elsewhere in the Pacific, so we have used the hypothetical composition of global average lower oceanic crust proposed by Peucker-Ehrenbrink et al. (2012) in our AFC models. While this has high Os (55 pg g^{-1}), moderate Re (427 pg g^{-1}) but unradiogenic $^{187}\text{Os}/^{188}\text{Os}$ (0.142), relative to upper crust, AFC models (Fig. 6a) show this also cannot satisfactorily explain the radiogenic $^{187}\text{Os}/^{188}\text{Os}$ of Galápagos basalts. Radiogenic in-growth of ^{187}Os for 10 Ma crust with MORB-like $^{187}\text{Os}/^{188}\text{Os}_i$ (0.127) would only cause a small increase in $^{187}\text{Os}/^{188}\text{Os}$ (to 0.1345), which is lower than the ratio observed in most of the basalts, including some with Os in excess of 50 pg g^{-1} (Fig. 6a).

We also used the composition of high Re/Os lower oceanic crust from the SW Indian Ridge (DSDP 735B; Blusztajn et al., 2000) in our AFC models (Fig. 6b). This contains 9 pg g^{-1} Os and 2153 pg g^{-1} Re, and is hence relatively evolved (Gannoun et al., 2016) so that the amount of ^{187}Os generated by radiogenic in-growth is large, and the $^{187}\text{Os}/^{188}\text{Os}$ of crust with an initial ratio of 0.127 increases over a 10 Ma time interval to 0.3205. While this high Re/Os lower oceanic crust can be used to satisfactorily model the range of Os and $^{187}\text{Os}/^{188}\text{Os}$ ratios in some basalts from western and southern Galápagos, contamination by crust of this composition cannot account for the combined high Os and radiogenic $^{187}\text{Os}/^{188}\text{Os}$ in the majority of samples (Fig. 6b). This is because in AFC models there is a trade-off between the rate of assimilation to fractionation (r_a) and the Os content of both the crust and magma: the amount of fractional crystallisation predicted by our models requires that, even for gabbros with $^{187}\text{Re}/^{188}\text{Os}$ as high as those reported by Blusztajn et al. (2000), any plausible contaminant for Galápagos basalts must have $>\sim 50 \text{ pg g}^{-1}$ Os (Fig. 6). The fact that the $^{187}\text{Os}/^{188}\text{Os}_{10\text{Ma}}$ ratio of the postulated crustal contaminant for NE Galápagos basalts is more radiogenic (0.25 to 0.3) and the Os content higher (50 to 100 pg g^{-1}) than observed in the limited number of analyses of gabbros from lower oceanic crust (Blusztajn et al., 2000; Dale et al., 2007; Peucker-Ehrenbrink et al., 2012) is an important finding from our study. We now explore mechanisms that might potentially cause an increase in the Re and Os contents of the crustal contaminant.

The origin of the $^{187}\text{Os}/^{188}\text{Os}$ variability of oceanic crust is not well understood (see Gannoun et al., 2016) but significant amounts of Re (up to 75%) may reside in silicate phases (Dale et al., 2009a) and cumulate magnetite (Richter et al., 1998). Sulfides (e.g. chalcopyrite, pentlandite, pyrrhotite, pyrite) are the major host of crustal Os ($>90\%$) and also some Re (Dale et al., 2009a), and variable assimilation of these minerals may well explain some of the Galápagos Re–Os data. Since magmatic sulfides have high Os but relatively low Re/Os, and unlikely to produce the elevated $^{187}\text{Os}/^{188}\text{Os}$ of a plausible contaminant, we suggest that the sulfides precipitated from S-rich hydrothermal fluids. Hydrothermal activity is evident in the upper parts of the oceanic crust – including in DSDP 504B (Bach et al., 2003) – and alteration affects up to 40% of gabbros (Nicolas et al., 2003).

According to Peucker-Ehrenbrink et al. (2003) ‘neither Holes 504B or 735B are representative of altered oceanic crust in general’ and it is therefore unsurprising that the published Re–Os data for these sites do not correspond to crust assimilated by Galápa-

gos basalts. In the light of there being no appropriate end member composition in the current $^{187}\text{Os}/^{188}\text{Os}$ oceanic crust database we used a series of hypothetical compositions. A best fit to the observed $^{187}\text{Os}/^{188}\text{Os}$ ratios of basalts from central, northeastern and eastern Galápagos was obtained in AFC models using a hypothetical, hydrothermal sulfide-rich gabbro with 100 pg g^{-1} Os, $^{187}\text{Os}/^{188}\text{Os}$ of 0.3, r_a values ranging from ~ 0.2 to 0.6 and 30 to 40% fractional crystallisation (Fig. 6a). If the Os content of the crust is only 50 pg g^{-1} , then the maximum r_a increases to 0.8 but the amount of fractional crystallisation decreases slightly to $<30\%$ (Fig. 6c). While the maximum estimated r_a for high-MgO Galápagos basalts is between 0.6 and 0.8, those with high $^{187}\text{Os}/^{188}\text{Os}$ from the west of the archipelago undergo less fractionation (20%) than those in the east (40%) for similar amounts of assimilation (Fig. 6a), i.e. crustal contamination is more sporadic but occurs at higher MgO contents and temperatures nearer the plume stem. The result of the model involving a contaminant with high Os (100 pg g^{-1}) is in agreement with AFC models which have shown that the amount of assimilation is limited by the thermal energy of the magma and for most cases maximum assimilation rates are attained very rapidly, i.e. at low amounts of fractional crystallisation (Bohrson and Spera, 2001). Our estimates of assimilation assume bulk crustal melting: selective melting of sulfides would reduce the amount of fractionation required only as long as the melt is under-saturated in this phase, which is not the case for Galápagos (Figs. 2 and S2).

Mixing curves between isotopically different Galápagos melts and lower crust in $^{187}\text{Os}/^{188}\text{Os}$ and $^{87}\text{Sr}/^{86}\text{Sr}$ space (Fig. 3) reveal that, even with a contaminant containing 100 pg g^{-1} Os, assimilation of $\sim 40\%$ highly-radiogenic oceanic crust would be required to explain the Os isotopic characteristics of Galápagos basalts with the most elevated $^{187}\text{Os}/^{188}\text{Os}$ and lowest $^{87}\text{Sr}/^{86}\text{Sr}$ ratios. This crust must also have a very high Re concentration, or at least have gained radiogenic ^{187}Os through alteration. The predicted amounts of contamination for some Galápagos basalts are high but are consistent with the findings of Kvassnes and Grove (2008) who showed that ascending parental MORB magmas are capable of melting significant amounts (50 wt.%) of gabbroic lower crust, while simultaneously crystallising olivine and subsequently plagioclase. We note that estimates of assimilation from Os in SW Indian Ridge MORB – which possess similarly radiogenic $^{187}\text{Os}/^{188}\text{Os}$ to Galápagos – give lower values of around 10% assimilation (Yang et al., 2013), but this is due to a model with only 15 pg g^{-1} Os in the melt and the most radiogenic lower crust value (0.467) from Blusztajn et al. (2000). We envisage that primitive Galápagos-plume related magmas are $\sim 75^\circ\text{C}$ hotter than MORB and, given reasonable residence times and magma chamber geometries, would be readily able to melt lower crust.

6.2. The importance of plume melt flux on $^{187}\text{Os}/^{188}\text{Os}$ of Galápagos basalts

Our findings show that the variability of $^{187}\text{Os}/^{188}\text{Os}$ in Galápagos is to a large extent regionally controlled and related to both mantle and crustal processes (Fig. 7). This relationship has not previously been observed in OIBs. The most crustally-contaminated Galápagos magmas occur where there is a low magmatic flux, i.e. where plume material is being dispersed laterally, and there is significantly less upwelling ($\sim 2 \text{ cm yr}^{-1}$) than at the plume stem ($\sim 7 \text{ cm yr}^{-1}$), such as at E. Santiago, Genovesa and Pinta (Figs. 1 and S5; Saal et al., 2000). Volcanoes in the west of the archipelago are built on the massive Galápagos Platform, which is constructed entirely of regionally extensive lava flows, and enormous volumes of plume derived magma have already passed through the crust by the time the central volcanoes (e.g. Fernandina) began their construction. The relatively low volumes

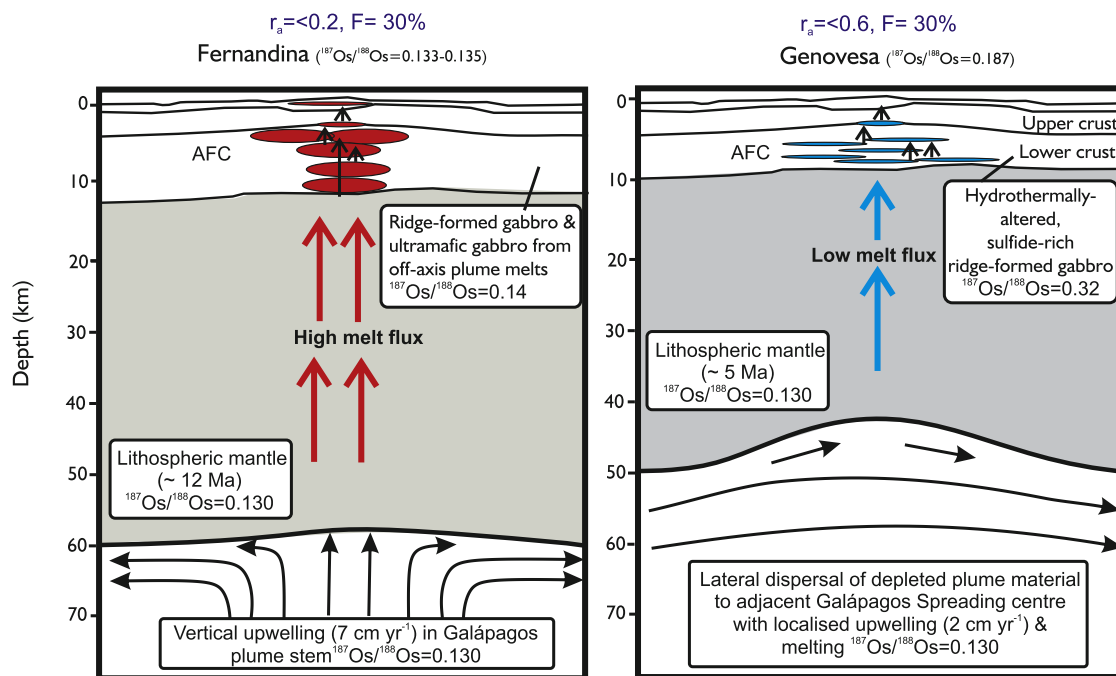


Fig. 7. Schematic illustrations to show the relationship between melt flux and $^{187}\text{Os}/^{188}\text{Os}$ beneath Fernandina and Genovesa which are located near and distal to the main zone of plume upwelling, respectively. The extent of crystal fractionation (F) and rate of assimilation to fractionation (r_a) are estimated from AFC models. $^{187}\text{Os}/^{188}\text{Os}$ data are from Table 1. Upwelling velocities are from U-series data (Saal et al., 2000). Lithospheric thickness estimates are from Gibson and Geist (2010).

of melt generated by relatively passive adiabatic decompression of plume material beneath the northern and eastern islands (Gibson et al., 2015) would encourage the development of small lower-crustal magma chambers with low volume to surface ratios. Magmatic plumbing systems involving a low flux of melt from the Galápagos plume are likely to be complex, with magmas following new ascent paths through the lithosphere, rather than previously established flow channels. These conditions would encourage assimilation of surrounding gabbro. Indeed, the elevated Os isotopic ratios of high-MgO Galápagos melts show that many were contaminated as soon as they began their migration through the crust, *i.e.* prior to undergoing extensive cooling and crystal fractionation. In this respect our findings differ from those of Saal et al. (2007) who used more-highly fractionated, plagioclase-saturated, MORB-like melt compositions to model the geochemical variations that might result from diffusive interaction of Galápagos melts with plagioclase in the lower crust.

Our $^{187}\text{Os}/^{188}\text{Os}$ data suggest that assimilation of oceanic crust by Galápagos plume-derived melts is sporadic on short length scales, *i.e.* individual volcanic centres. The regional variations in $^{187}\text{Os}/^{188}\text{Os}$ are best accounted for by differences in the extent of assimilation and fractional crystallisation. The observation that Galápagos basalts with the least enriched Sr-, Nd- and Pb-isotopic ratios have undergone the greatest amounts of crustal contamination is due to: (i) the off axis location of the Galápagos plume stem; and (ii) relatively thin lithosphere above the site of channelled plume flow to the ridge (Gibson et al., 2015). It is the low melt flux that causes magmas to stall, cool and fractionate, and this explains the lack of lavas with primitive major-element compositions. Nevertheless, our study has shown that while assimilation of hydrothermally-altered lower crust increases $^{187}\text{Os}/^{188}\text{Os}$ ratios of Galápagos basalts, Sr-, Nd- and Pb-isotopic ratios are relatively unaffected by this process (because of the relatively small isotopic difference between primary melt and contaminant) and retain the signatures of their mantle source regions (*cf.* Fig. 3).

7. Comparison of Galápagos Re–Os data with global OIBs

In general, a broad positive correlation exists between $^{187}\text{Os}/^{188}\text{Os}$ of global OIBs with high Os ($>50 \text{ pg g}^{-1}$) and the age of the underlying lithosphere (Fig. 8). For OIBs formed on old lithosphere, such as Hawaii, Canaries and Cook Austral, the high $^{187}\text{Os}/^{188}\text{Os}$ could be due to either: (i) older, thicker lithosphere limiting the amount of adiabatic decompression melting in the underlying mantle plume and therefore enhancing the effect of any pyroxenite melting relative to peridotite, or (ii) assimilation of ‘old’ crust with more radiogenic $^{187}\text{Os}/^{188}\text{Os}$. In Fig. 8 it is clear that some high Os Galápagos basalts have more radiogenic $^{187}\text{Os}/^{188}\text{Os}$ than basalts formed on young lithosphere ($<50 \text{ Ma}$) such as at Iceland, the Azores and Pitcairn, and as discussed above we attribute this to assimilation of crust during relatively early stages of crystallisation at Galápagos.

While the $^{187}\text{Os}/^{188}\text{Os}$ ratios of oceanic crust are typically assumed to correlate with age, due to decay of ^{187}Re , the elevated $^{187}\text{Os}/^{188}\text{Os}$ ratios of some recent Galápagos basalts are testimony to the assimilation of young ($<10 \text{ Ma}$), hydrothermal sulfide-bearing, Re- and Os-rich lower oceanic crust. Our AFC models suggest that this has a more radiogenic Os isotopic signature than previously supposed in studies of oceanic basalts, which have assumed $^{187}\text{Os}/^{188}\text{Os}$ ratios of fresh gabbro for lower oceanic crust, *e.g.* Yang et al. (2013). This finding has fundamental implications for how Re–Os data are interpreted. For example, the involvement of high Re/Os recycled ancient mafic components (eclogite/pyroxenite) in the convecting mantle to explain the radiogenic $^{187}\text{Os}/^{188}\text{Os}$ of many Os-rich global OIBs (*e.g.* Lassiter and Hauri, 1998; Skovgaard et al., 2001; Class et al., 2009; Day et al., 2009) need not be so strongly invoked if assimilation of even young oceanic crust may overprint the Os isotopic signature of magmas with Os contents $\leq 100 \text{ pg g}^{-1}$. What remains uncertain is whether or not gabbro with radiogenic $^{187}\text{Os}/^{188}\text{Os}$ is restricted to hydrothermally-altered, sulfide-rich crust that formed at spreading centres or may also occur in plume-formed crust generated away from mid-ocean ridges. The marked increase in Os isotopic ratios with distance from the upwelling plume stem

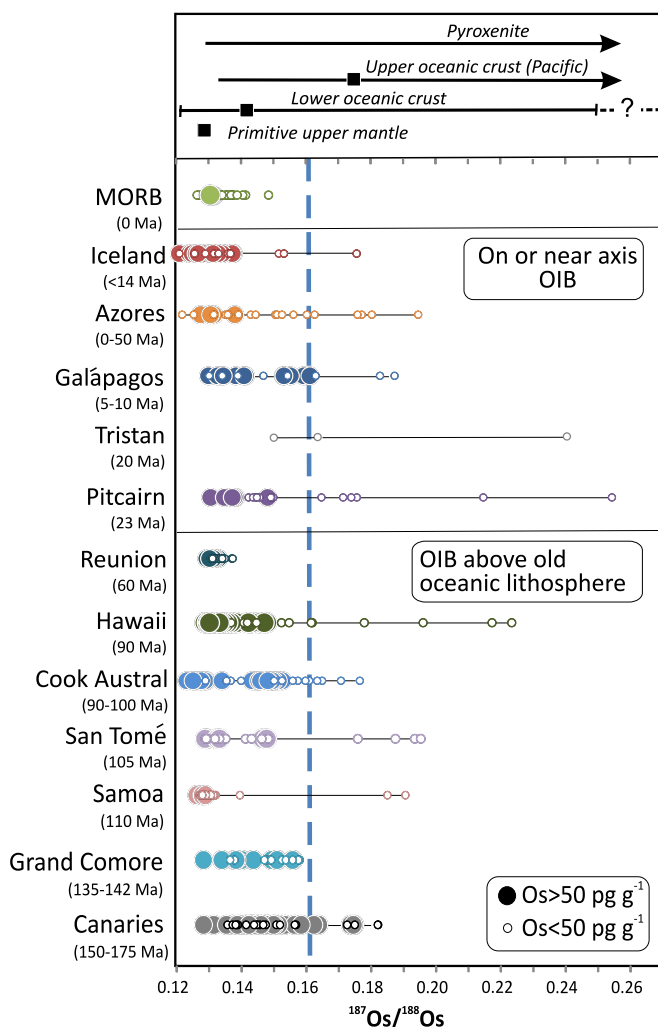


Fig. 8. Comparison of $^{187}\text{Os}/^{188}\text{Os}$ in global MORB and OIBs according to age of the underlying lithosphere. Basalts are divided into low Os and high Os groups based on a threshold of 50 pg g^{-1} , the canonical maximum value used to filter effects of crustal contamination. Note the general increase in range of $^{187}\text{Os}/^{188}\text{Os}$ in basalts with $>50 \text{ pg g}^{-1}$ and age of the underlying lithosphere. Galápagos basalts with $>50 \text{ pg g}^{-1}$ Os are unusual in that they have relatively high $^{187}\text{Os}/^{188}\text{Os}$ given the young age of the underlying lithosphere (as indicated by thick dashed line). Data sources are given in a Supplementary File.

that we observe in Galápagos has not been reported from other global suites of oceanic basalts and may depend on the near-ridge setting of Galápagos and also the unique widespread distribution of active volcanism in the archipelago. Nevertheless, changes in Os isotopic ratios related to temporal variations in melt flux have been inferred for both Iceland (Skovgaard et al., 2001; Debaille et al., 2009) and Hawaii (Gaffney et al., 2005).

Galápagos basalts are exceptional in that, although erupted in a near-ridge setting, they have radiogenic $^{187}\text{Os}/^{188}\text{Os}$ at relatively high MgO and Os contents (100 pg g^{-1} ; Figs. 8 and 9), which suggests contamination occurs at an earlier stage in crustal processing than has been identified in many other OIBs. The volume flux of melt estimated for the present-day Galápagos plume ($2.8 \pm 1.6 \text{ m}^3/\text{s}$) is less than half that of Hawaii ($5.0 \pm 3.7 \text{ m}^3/\text{s}$) and Iceland ($9.2 \pm 6.7 \text{ m}^3/\text{s}$; Sallarès and Charvis, 2003) and we suggest this controls the introduction of crustal Os into OIBs with moderate to high Os contents. Furthermore, the Galápagos plume generates less melt than near-axis hotspots such as the Azores, Pitcairn and Iceland because it impacts beneath thicker lithosphere. An important first order observation is that many Galápagos basalts with radiogenic $^{187}\text{Os}/^{188}\text{Os}$ were erupted from volcanoes located dis-

tal to the plume stem (i.e. region of greatest upwelling; Figs. 1 and S5) and we anticipate these will have magma chambers supplied by the lowest melt flux. Moreover, the distinct isotopic signature (White et al., 1993) and olivine chemistry (Vidito et al., 2013) of each Galápagos volcano suggest they are each underlain by a relatively small magma chamber in comparison to Hawaii and Iceland.

8. Conclusions

Our new Re–Os isotopic data for Galápagos basalts reveal a large systematic regional variation in $^{187}\text{Os}/^{188}\text{Os}$ composition, which represents both mantle and crustal processes. Basalts recently erupted near the western margin of the Galápagos platform (Fernandina and Roca Redonda) and at the leading edge of the hotspot track are the least radiogenic ($^{187}\text{Os}/^{188}\text{Os} \sim 0.130$). This is consistent with the presence of a mantle reservoir in the Galápagos plume resembling the “C”-like global plume component. In Os–Pb isotopic space, basalts from Floreana fall on a mixing curve between global “C” and HIMU mantle reservoirs and confirm that ancient recycled crust with elevated $^{187}\text{Os}/^{188}\text{Os}$ and $^{206}\text{Pb}/^{204}\text{Pb}$ is melting in the southern part of the upwelling Galápagos plume (Harpp et al., 2014). These findings concur with previous studies that have suggested the Galápagos plume is compositionally zoned (e.g. White et al., 1993; Hoernle et al., 2000).

A key finding is that basalts with radiogenic $^{187}\text{Os}/^{188}\text{Os}$ were erupted from volcanoes distal to the main zone of Galápagos plume upwelling, where plume material is laterally dispersed, i.e. in central and northeast parts of the archipelago. There is no correlation of $^{187}\text{Os}/^{188}\text{Os}$ with purported lithological variations in the Galápagos plume (Vidito et al., 2013) but positive correlations of $^{187}\text{Os}/^{188}\text{Os}$ with indices of crystal fractionation (Os, Ni, Cr and MgO) suggest that large variations in $^{187}\text{Os}/^{188}\text{Os}$ are related to lithospheric processing, involving assimilation of lower oceanic crust during crystal fractionation, rather than mantle melting. In order to account for the observed variability in Os isotopic ratios we suggest that ridge-formed oceanic crust underlying Galápagos is enriched in radiogenic ^{187}Os , probably in the form of Os- and Re-rich hydrothermal sulfides. Such material, or simply older oceanic crustal material, may also explain the elevated $^{187}\text{Os}/^{188}\text{Os}$ of some other OIBs, including those that have been linked to melting of ancient pyroxenitic material.

The potential of Galápagos mantle plume-derived melts to assimilate Pacific lower crust is influenced by the melt flux and crustal residence times, which themselves are dependent upon the density difference between magma and crust. The lower melt flux of the Galápagos plume relative to the Hawaiian and Icelandic plumes may account for the early onset of contamination (expressed by MgO and Os contents) in ascending melts. Our findings from Galápagos show that, provided the rate of assimilation to crystal fractionation is low (<0.2), a threshold bulk-rock Os content of $30\text{--}50 \text{ pg g}^{-1}$ is an appropriate contamination filter for melts which have ascended through the estimated young lower oceanic crust of Peucker-Ehrenbrink et al. (2012). If, however, the oceanic crust has a greater concentration of Os, higher $^{187}\text{Os}/^{188}\text{Os}$ ratio, or the rate of assimilation to crystal fractionation is much higher, then the contamination filter threshold should be set at a greater Os content.

The causes of the large variability in $^{187}\text{Os}/^{188}\text{Os}$ that we have identified in Galápagos basalts have important implications for $^{187}\text{Os}/^{188}\text{Os}$ in global OIBs associated with weak mantle plumes (e.g. those at the end of long-lived hot spot tracks) and also off-axis mantle plumes, such as Tristan da Cunha, Bouvet, Crozet and St Helena. We urge caution in attributing radiogenic $^{187}\text{Os}/^{188}\text{Os}$ in basalts, especially associated with these hotspots, solely to lithological heterogeneity (recycled oceanic crust) in the convecting mantle, particularly in low Os basalts.

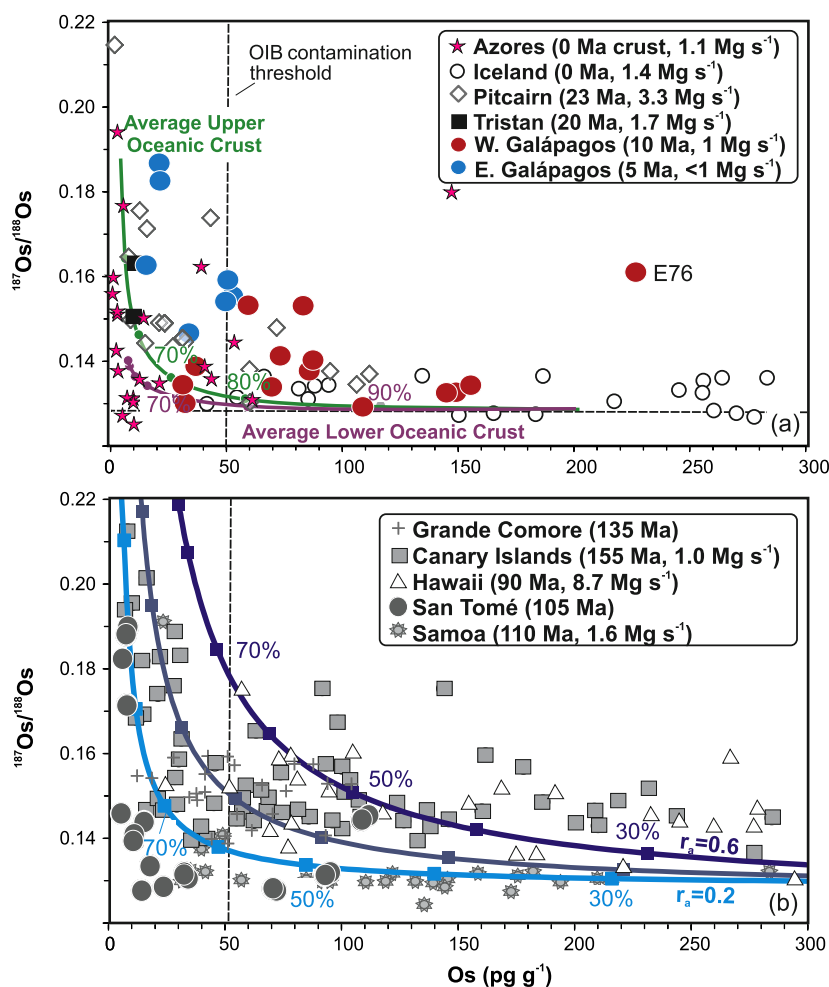


Fig. 9. Assimilation fractional crystallisation curves for: a) basalts erupted on young oceanic crust with typical average zero-aged upper and lower oceanic crust; and b) basalts erupted on old oceanic crust with $^{187}\text{Os}/^{188}\text{Os}$ of average lower oceanic crust age corrected to 150 Ma (0.221) and $\text{Os} = 55 \text{ pg g}^{-1}$ (Blusztajn et al., 2000). The threshold of 30–50 pg g^{-1} Os below which contamination is thought to exert a significant influence on the $^{187}\text{Os}/^{188}\text{Os}$ of oceanic basalts (Reisberg et al., 1993) is shown for reference. Data sources are the same as Fig. 3. Data sources for ages of oceanic crust and buoyancy flux data beneath different islands are given in a Supplementary file.

Acknowledgements

We thank the Galápagos National Park authorities for permission to collect samples in the Archipelago. We are grateful to Julia Griffin and Iris Buisman for help with electron microprobe analyses and Geoff Nowell for assistance with Sr, Nd and Pb isotope determinations. We thank Jason Harvey and Cornelia Class for their thorough and constructive reviews of an earlier draft of this manuscript, and Bernard Marty for his very efficient editorial handling of our paper. The research was funded by NERC RG57434 (SAG) and EAR-1145271 (DG).

Appendix A. Supplementary material

Supplementary material related to this article can be found online at <http://dx.doi.org/10.1016/j.epsl.2016.05.021>.

References

- Allègre, C.J., Luck, J.-M., 1980. Osmium isotopes as petrogenetic and geological tracers. *Earth Planet. Sci. Lett.* 48 (1), 148–154. [http://dx.doi.org/10.1016/0012-821X\(80\)90177-6](http://dx.doi.org/10.1016/0012-821X(80)90177-6).
- Bach, W., Peucker-Ehrenbrink, B., Hart, S.R., Blusztajn, J.S., 2003. Geochemistry of hydrothermally altered oceanic crust: DSDP/ODP Hole 504B – implications for seawater-crust exchange budgets and Sr- and Pb-isotopic evolution of the mantle. *Geochem. Geophys. Geosyst.* 4 (3), 8904. <http://dx.doi.org/10.1029/2002GC000419>.
- Beattie, P., Ford, C., Russell, D., 1991. Partition coefficients for olivine-melt and orthopyroxene-melt systems. *Contrib. Mineral. Petrol.* 109 (2), 212–224. <http://dx.doi.org/10.1007/BF00306480>.
- Bennett, V.C., Norman, M.D., Garcia, M.O., 2000. Rhenium and platinum group element abundances correlated with mantle source components in Hawaiian picrites: sulphides in the plume. *Earth Planet. Sci. Lett.* 183 (3–4), 513–526. [http://dx.doi.org/10.1016/S0012-821X\(00\)00295-8](http://dx.doi.org/10.1016/S0012-821X(00)00295-8).
- Blusztajn, J., Hart, S.R., Ravizza, G., Dick, H.J.B., 2000. Platinum-group elements and Os isotopic characteristics of the lower oceanic crust. *Chem. Geol.* 168 (1–2), 113–122. [http://dx.doi.org/10.1016/S0009-2541\(00\)00186-8](http://dx.doi.org/10.1016/S0009-2541(00)00186-8).
- Bohrson, W.A., Spera, F.J., 2001. Energy-constrained open-system magmatic processes II: application of energy-constrained assimilation-fractional crystallization (EC-AFC) model to magmatic systems. *J. Petrol.* 42 (5), 1019–1041. <http://dx.doi.org/10.1093/ptrology/42.5.1019>.
- Burton, K.W., Schiano, P., Birck, J.-L., Allègre, C.J., Rehkämper, M., Halliday, A.N., Dawson, J.B., 2000. The distribution and behaviour of rhenium and osmium amongst mantle minerals and the age of the lithospheric mantle beneath Tanzania. *Earth Planet. Sci. Lett.* 183 (1–2), 93–106. [http://dx.doi.org/10.1016/S0012-821X\(00\)00259-4](http://dx.doi.org/10.1016/S0012-821X(00)00259-4).
- Burton, K.W., Gannoun, A., Birck, J.-L., Allègre, C.J., Schiano, P., Clocchiatti, R., Alard, O., 2002. The compatibility of rhenium and osmium in natural olivine and their behaviour during mantle melting and basalt genesis. *Earth Planet. Sci. Lett.* 198 (1–2), 63–76. [http://dx.doi.org/10.1016/S0012-821X\(02\)00518-6](http://dx.doi.org/10.1016/S0012-821X(02)00518-6).
- Canales, J.P., Ito, G., Detrick, R.S., Sinton, J.M., 2002. Crustal thickness along the western Galápagos spreading center and the compensation of the Galápagos hotspot swell. *Earth Planet. Sci. Lett.* 203 (1), 311–327.
- Class, C., Goldstein, S.L., Shirey, S.B., 2009. Osmium isotopes in Grande Comore lavas: a new extreme among a spectrum of EM-type mantle endmembers. *Earth Planet. Sci. Lett.* 284 (1–2), 219–227. <http://dx.doi.org/10.1016/j.epsl.2009.04.031>.

- Dale, C.W., Gannoun, A., Burton, K.W., Argles, T.W., Parkinson, I.J., 2007. Rhenium–osmium isotope and elemental behaviour during subduction of oceanic crust and the implications for mantle recycling. *Earth Planet. Sci. Lett.* 253 (1–2), 211–225. <http://dx.doi.org/10.1016/j.epsl.2006.10.029>.
- Dale, C.W., Burton, K.W., Pearson, D.G., Gannoun, A., Alard, O., Argles, T.W., Parkinson, I.J., 2009a. Highly siderophile element behaviour accompanying subduction of oceanic crust: whole rock and mineral-scale insights from a high-pressure terrrain. *Geochim. Cosmochim. Acta* 73 (5), 1394–1416. <http://dx.doi.org/10.1016/j.gca.2008.11.036>.
- Dale, C.W., Pearson, D.G., Starkey, N.A., Stuart, F.M., Ellam, R.M., Larsen, L.M., Fitton, J.G., Macpherson, C.G., 2009b. Osmium isotopes in Baffin Island and West Greenland picrites: implications for the $^{187}\text{Os}/^{188}\text{Os}$ composition of the convecting mantle and the nature of high $^3\text{He}/^4\text{He}$ mantle. *Earth Planet. Sci. Lett.* 278 (3–4), 267–277. <http://dx.doi.org/10.1016/j.epsl.2008.12.014>.
- Danyushevsky, L.V., Plechov, P., 2011. Petrolog3: integrated software for modeling crystallization processes. *Geochim. Geophys. Geosyst.* 12 (7), Q07021. <http://dx.doi.org/10.1029/2011GC003516>.
- Day, J.M.D., Pearson, D.G., Macpherson, C.G., Lowry, D., Carracedo, J.-C., 2009. Pyroxenite-rich mantle formed by recycled oceanic lithosphere: oxygen–osmium isotope evidence from Canary Island lavas. *Geology* 37 (6), 555–558.
- Day, J.M.D., Pearson, D.G., Macpherson, C.G., Lowry, D., Carracedo, J.C., 2010. Evidence for distinct proportions of subducted oceanic crust and lithosphere in HIMU-type mantle beneath El Hierro and La Palma, Canary Islands. *Geochim. Cosmochim. Acta* 74 (22), 6565–6589. <http://dx.doi.org/10.1016/j.gca.2010.08.021>.
- Debaille, V., Trønnes, R.G., Brandon, A.D., Waight, T.E., Graham, D.W., Lee, C.-T.A., 2009. Primitive off-rift basalts from Iceland and Jan Mayen: Os-isotopic evidence for a mantle source containing enriched subcontinental lithosphere. *Geochim. Cosmochim. Acta* 73 (11), 3423–3449. <http://dx.doi.org/10.1016/j.gca.2009.03.002>.
- Eisele, J., Sharma, M., Galer, S.J.G., Blichert-Toft, J., Devey, C.W., Hofmann, A.W., 2002. The role of sediment recycling in EM-1 inferred from Os, Pb, Hf, Nd, Sr isotope and trace element systematics of the Pitcairn hotspot. *Earth Planet. Sci. Lett.* 196 (3–4), 197–212. [http://dx.doi.org/10.1016/S0012-821X\(01\)00601-X](http://dx.doi.org/10.1016/S0012-821X(01)00601-X).
- Feighner, M.A., Richards, M.A., 1994. Lithospheric structure and compensation mechanisms of the Galápagos Archipelago. *J. Geophys. Res., Solid Earth* 99 (B4), 6711–6729.
- Gaffney, A.M., Nelson, B.K., Reisberg, L., Eiler, J., 2005. Oxygen–osmium isotope systematics of West Maui lavas: a record of shallow-level magmatic processes. *Earth Planet. Sci. Lett.* 239 (1–2), 122–139. <http://dx.doi.org/10.1016/j.epsl.2005.07.027>.
- Gannoun, A., Burton, K.W., Parkinson, I.J., Alard, O., Schiano, P., Thomas, L.E., 2007. The scale and origin of the osmium isotope variations in mid-ocean ridge basalts. *Earth Planet. Sci. Lett.* 259 (3–4), 541–556. <http://dx.doi.org/10.1016/j.jepsl.2007.05.014>.
- Gannoun, A., Burton, K.W., Day, J.M.D., Harvey, J., Schiano, P., Parkinson, I., 2016. Highly siderophile element and Os isotope systematics of volcanic rocks at divergent and convergent plate boundaries and in intraplate settings. *Rev. Mineral. Geochem.* 81 (1), 651–724. <http://dx.doi.org/10.2138/rmg.2016.81.11>.
- Geist, D.J., Naumann, T., Larson, P., 1998. Evolution of Galápagos magmas: mantle and crustal fractionation without assimilation. *J. Petrol.* 39 (5), 953–971.
- Geist, D.J., Fornari, D.J., Kurz, M.D., Harpp, K.S., Soule, A., Perfit, M., Koleszar, A.M., 2006. Submarine Fernandina: magmatism at the leading edge of the Galápagos hot spot. *Geochem. Geophys. Geosyst.* 7. <http://dx.doi.org/10.1029/2006GC001290>.
- Geist, D.J., Snell, H., Snell, H., Goddard, C., Kurz, M.D., 2014. A palaeogeographic model of Galápagos Islands and biogeographical and evolutionary implications. In: *The Galápagos: a Natural Laboratory for the Earth Sciences*. In: AGU Monograph, pp. 145–166.
- Gibson, S.A., Geist, D.J., 2010. Geochemical and geophysical mapping of lithospheric thickness variations beneath Galápagos. *Earth Planet. Sci. Lett.* 300, 275–286. <http://dx.doi.org/10.1016/j.epsl.2010.10.002>.
- Gibson, S.A., Geist, D.J., Day, J.A., Dale, C.W., 2012. Short wavelength heterogeneity in the Galápagos plume: evidence from compositionally-diverse basalts on Isla Santiago. *Geochem. Geophys. Geosyst.* <http://dx.doi.org/10.1029/2012GC004244>.
- Gibson, S.A., Geist, D.J., Richards, M.A., 2015. Mantle plume capture and outflow during Galápagos plume-ridge interaction. *Geochem. Geophys. Geosyst.* <http://dx.doi.org/10.1002/2015GC005723>.
- Harpp, K., Fornari, D., Geist, D.J., Kurz, M.D., 2014. The geology and geochemistry of Isla Floreana, Galápagos: a different type of late stage ocean island volcanism. In: *Galápagos Nat. Lab. Earth Sci. In: AGU Monogr.*, vol. 204, pp. 71–118.
- Harpp, K.S., White, W.M., 2001. Tracing a mantle plume: isotopic and trace element variations of Galápagos seamounts. *Geochem. Geophys. Geosyst.* 2. <http://dx.doi.org/10.1029/2000GC000137>.
- Hart, S.R., Blusztajn, J., Dick, H.J.B., Meyer, P.S., Muehlenbachs, K., 1999. The fingerprint of seawater circulation in a 500-meter section of ocean crust gabbros. *Geochim. Cosmochim. Acta* 63 (23–24), 4059–4080. [http://dx.doi.org/10.1016/S0016-7037\(99\)00309-9](http://dx.doi.org/10.1016/S0016-7037(99)00309-9).
- Harvey, J., Dale, C.W., Gannoun, A., Burton, K.W., 2011. Osmium mass balance in peridotite and the effects of mantle-derived sulphides on basalt petrogenesis. *Geochim. Cosmochim. Acta* 75 (19), 5574–5596. <http://dx.doi.org/10.1016/j.gca.2011.07.001>.
- Hauri, E.H., Lassiter, J.C., DePaolo, D.J., 1996. Osmium isotope systematics of drilled lavas from Mauna Loa, Hawaii. *J. Geophys. Res., Solid Earth* 101 (B5), 11793–11806. <http://dx.doi.org/10.1029/95JB03346>.
- Hoernle, K.A., Werner, R., Morgan, J.P., Garbe, S., Bryce, J., Mrazek, J., 2000. Existence of complex spatial zonation in the Galápagos plume. *Geology* 28 (5), 435–438.
- Jackson, M.G., Shirey, S.B., 2011. Re–Os isotope systematics in Samoan shield lavas and the use of Os-isotopes in olivine phenocrysts to determine primary magmatic compositions. *Earth Planet. Sci. Lett.* 312 (1–2), 91–101. <http://dx.doi.org/10.1016/j.epsl.2011.09.046>.
- Kurz, M.D., Curtice, J., Fornari, D., Geist, D.J., Moreira, M., 2009. Primitive neon from the center of the Galápagos hotspot. *Earth Planet. Sci. Lett.* 286 (1–2), 23–34.
- Kvassnes, A.J.S., Grove, T.L., 2008. How partial melts of mafic lower crust affect ascending magmas at oceanic ridges. *Contrib. Mineral. Petrol.* 156 (1), 49–71. <http://dx.doi.org/10.1007/s00410-007-0273-x>.
- Lassiter, J.C., Hauri, E.H., 1998. Osmium-isotope variations in Hawaiian lavas: evidence for recycled oceanic lithosphere in the Hawaiian plume. *Earth Planet. Sci. Lett.* 164 (3–4), 483–496. [http://dx.doi.org/10.1016/S0012-821X\(98\)00240-4](http://dx.doi.org/10.1016/S0012-821X(98)00240-4).
- Levasseur, S., Birck, J.-L., Allègre, C.J., 1998. Direct measurement of femtomoles of osmium and the $^{187}\text{Os}/^{186}\text{Os}$ ratio in seawater. *Science* 282 (5387), 272–274. <http://dx.doi.org/10.1126/science.282.5387.272>.
- Meisel, T., Walker, R.J., Irving, A.J., Lorand, J.-P., 2001. Osmium isotopic compositions of mantle xenoliths: a global perspective. *Geochim. Cosmochim. Acta* 65 (8), 1311–1323. [http://dx.doi.org/10.1016/S0016-7037\(00\)00566-4](http://dx.doi.org/10.1016/S0016-7037(00)00566-4).
- Nicolas, A., Mainprice, D., Boudier, F., 2003. High-temperature seawater circulation throughout crust of oceanic ridges: a model derived from the Oman ophiolites. *J. Geophys. Res., Solid Earth* 108 (B8), 2371. <http://dx.doi.org/10.1029/2002JB002094>.
- Nishimura, K., 2012. A mathematical model of trace element and isotopic behavior during simultaneous assimilation and imperfect fractional crystallization. *Contrib. Mineral. Petrol.* 164 (3), 427–440. <http://dx.doi.org/10.1007/s00410-012-0745-5>.
- Peterson, M.E., Saal, A.E., Nakamura, E., Kitagawa, H., Kurz, M.D., Koleszar, A.M., 2014. Origin of the “ghost plagioclase” signature in Galápagos melt inclusions: new evidence from Pb isotopes. *J. Petrol.* <http://dx.doi.org/10.1093/ptrology/egu054>.
- Peucker-Ehrenbrink, B., Bach, W., Hart, S.R., Blusztajn, J.S., Abbruzzese, T., 2003. Rhenium–osmium isotope systematics and platinum group element concentrations in oceanic crust from DSDP/ODP sites 504 and 417/418. *Geochem. Geophys. Geosyst.* 4 (7). <http://dx.doi.org/10.1029/2002GC000414>.
- Peucker-Ehrenbrink, B., Hanghøj, K., Atwood, T., Kelemen, P.B., 2012. Rhenium–osmium isotope systematics and platinum group element concentrations in oceanic crust. *Geology* 40 (3), 199–202. <http://dx.doi.org/10.1130/G32431.1>.
- Reisberg, L., Zindler, A., Marcantonio, F., White, W., Wyman, D., Weaver, B., 1993. Os isotope systematics in ocean island basalts. *Earth Planet. Sci. Lett.* 120 (3–4), 149–167. [http://dx.doi.org/10.1016/0012-821X\(93\)90236-3](http://dx.doi.org/10.1016/0012-821X(93)90236-3).
- Richards, M., Contreras-Reyes, E., Lithgow-Bertelloni, C., Ghiorso, M., Stixrude, L., 2013. Petrological interpretation of deep crustal intrusive bodies beneath oceanic hotspot provinces. *Geochem. Geophys. Geosyst.* 14 (3), 604–619. <http://dx.doi.org/10.1029/2012GC004448>.
- Righter, K., Chesley, J.T., Geist, D., Ruiz, J., 1998. Behavior of Re during magma fractionation: an example from Volcán Alcedo, Galápagos. *J. Petrol.* 39 (4), 785–795. <http://dx.doi.org/10.1093/ptrolyj/39.4.785>.
- Saal, A.E., Kurz, M.D., Hart, S., Blusztajn, J.S., Lane, G.D., Sims, K., Geist, D.J., 2000. U series isotopic variability in Galápagos lavas, evidence of a mildly buoyant plume. In: *AGU Fall Meet. Abstr.* V22C–03.
- Saal, A.E., Kurz, M.D., Hart, S.R., Blusztajn, J.S., Blichert-Toft, J., Liang, Y., Geist, D.J., 2007. The role of lithospheric gabbros on the composition of Galápagos lavas. *Earth Planet. Sci. Lett.* 257, 391–406.
- Sallarès, V., Charvis, P., 2003. Crustal thickness constraints on the geodynamic evolution of the Galápagos volcanic province. *Earth Planet. Sci. Lett.* 214 (3–4), 545–559. [http://dx.doi.org/10.1016/S0012-821X\(03\)00373-X](http://dx.doi.org/10.1016/S0012-821X(03)00373-X).
- Sallarès, V., Charvis, P., Flueh, E.R., Bialas, J., 2003. Seismic structure of Cocos and Malpelo Volcanic Ridges and implications for hot spot-ridge interaction. *J. Geophys. Res., Solid Earth* 108 (B12). <http://dx.doi.org/10.1029/2003JB002431>.
- Skovgaard, A.C., Storey, M., Baker, J., Blusztajn, J., Hart, S.R., 2001. Osmium–oxygen isotopic evidence for a recycled and strongly depleted component in the Iceland mantle plume. *Earth Planet. Sci. Lett.* 194 (1–2), 259–275. [http://dx.doi.org/10.1016/S0012-821X\(01\)00549-0](http://dx.doi.org/10.1016/S0012-821X(01)00549-0).
- Tejada, M.L.G., et al., 2015. Re–Os isotope and platinum group elements of a Focal Zone mantle source, Louisville Seamounts Chain, Pacific ocean. *Geochem. Geophys. Geosyst.* 16, 486–504.
- Vidito, C., Herzberg, C., Gazel, E., Geist, D., Harpp, K., 2013. Lithological structure of the Galápagos plume. *Geochem. Geophys. Geosyst.* 14 (10), 4214–4240. <http://dx.doi.org/10.1002/ggge.20270>.

- Villagómez, D.R., Toomey, D.R., Geist, D.J., Hooft, E.E.E., Solomon, S.C., 2014. Mantle flow and multistage melting beneath the Galápagos hotspot revealed by seismic imaging. *Nat. Geosci.* <http://dx.doi.org/10.1038/ngeo2062>.
- White, W.M., McBirney, A.R., Duncan, R.A., 1993. Petrology and geochemistry of the Galápagos Islands – portrait of a pathological mantle plume. *J. Geophys. Res., Solid Earth* 98 (B11), 19533–19563.
- Widom, E., Shirey, S.B., 1996. Os isotope systematics in the Azores: implications for mantle plume sources. *Earth Planet. Sci. Lett.* 142 (3–4), 451–465. [http://dx.doi.org/10.1016/0012-821X\(96\)00111-2](http://dx.doi.org/10.1016/0012-821X(96)00111-2).
- Yang, A.Y., Zhao, T.-P., Zhou, M.-F., Deng, X.-G., Wang, G.-Q., Li, J., 2013. Os isotopic compositions of MORBs from the ultra-slow spreading Southwest Indian Ridge: constraints on the assimilation and fractional crystallization (AFC) processes. *Lithos* 179, 28–35. <http://dx.doi.org/10.1016/j.lithos.2013.07.020>.